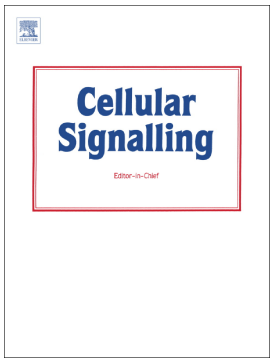

Urokinase receptor deficiency results in EGFR-mediated failure to transmit signals for cell survival and neurite formation in mouse neuroblastoma cells

K.D. Rysenkova, P.S. Klimovich, A.A. Shmakova, M.N. Karagyaur, K.A. Ivanova, N.A. Aleksandrushkina, V.A. Tkachuk, K.A. Rubina, E.V. Semina

PII: S0898-6568(20)30218-7

DOI: https://doi.org/10.1016/j.cellsig.2020.109741

Reference: CLS 109741

To appear in: *Cellular Signalling*

Received date: 12 May 2020

Revised date: 14 August 2020

Accepted date: 14 August 2020

Please cite this article as: K.D. Rysenkova, P.S. Klimovich, A.A. Shmakova, et al., Urokinase receptor deficiency results in EGFR-mediated failure to transmit signals for cell survival and neurite formation in mouse neuroblastoma cells, *Cellular Signalling* (2020), https://doi.org/10.1016/j.cellsig.2020.109741

Urokinase receptor deficiency results in EGFR-mediated failure to transmit signals for cell survival and neurite formation in mouse neuroblastoma cells

Rysenkova K.D.[1,2], Klimovich P.S.[1], Shmakova A.A.[1], Karagyaur M.N.[4], Ivanova K.A.[2], Aleksandrushkina N.A.[2,4], Tkachuk V.A.[1,2], Rubina K.A.[3*], Semina E.V.[1,2]

[1]Laboratory of Molecular Endocrinology, Institute of Experimental Cardiology, Federal State Budgetary Organization National Cardiology Research Center Ministry of Health of the Russian Federation, Moscow, Russia

[2]Laboratory of Gene and Cell Technologies, Faculty of Medicine, Lomonosov Moscow State University, Moscow, Russia

[3]Laboratory of Morphogenesis and Tissue Reparation, Faculty of Medicine, Lomonosov Moscow State University, Moscow, Russia

[4]Institute of Regenerative Medicine, Medical Research and Education Center, Lomonosov Moscow State University, Moscow, Russian Federation

*Corresponding author: rkseniya@mail.ru

Abstract

Urokinase-type plasminogen activator uPA and its receptor (uPAR) are the central players in extracellular matrix proteolysis, which facilitates cancer invasion and metastasis. EGFR is one of the important components of uPAR interactome. uPAR/EGFR interaction controls signaling pathways that regulate cell survival, proliferation and migration. We have previously established that uPA binding to uPAR stimulates neurite elongation in neuroblastoma cells, while blocking uPA uPAR interaction induces neurite branching and new neurite formation. Here we demonstrate that blocking the uPA binding to uPAR with anti-uPAR antibody decreases the level of pEGFR ~~(Y1068)~~ and its downstream pERK1/2, ~~(T202+Y204),,~~ but does increase phosphorylation of Akt, ~~(S473),~~, p38 ~~(Y180/182)~~ and c-Src ~~(Y412). The obtained results implicate uPAR/EGFR signaling axis as an important effector of the apoptotic pathway in Neuro2a cells. Long.~~ Since long-term uPAR blocking results in a ~~dramatic loss of NeuN expression (a marker of neuron differentiation) and a decline in cell survival due to~~ severe DNA damage, accompanied by PARP-1 proteolysis and Neuro2a cell death, we surmise that Akt, p38 and c-Src activation transmits a pro-apoptotic signal, rather than a survival.

Serum deprivation resulting in enhanced neuritogenesis is accompanied by an upregulated uPAR mRNA expression, while EGFR mRNA remains unchanged. EGFR activation by EGF stimulates neurite growth only in uPAR-overexpressing cells but not in control or uPAR-deficient cells. In addition, AG1478-mediated inhibition of EGFR activity

impedes neurite growth in control and uPAR-deficient cells, but not in uPAR-overexpressing cells. Altogether these data implicate uPAR as an important regulator of EGFR and ERK1/2 signaling, representing a novel mechanism which implicates urokinase system in neuroblastoma cell survival and differentiation.

Key words: urokinase plasminogen activator receptor, neuroblastoma, Neuro2a, EGFR, apoptosis, neuritogenesis.

Introduction

Neuroblastoma is the most common infancy cancer with an uncertain mechanism of spontaneous regression or differentiation [1]. Neoplastic transformation is considered to be induced by alterations in molecular signaling pathways during maturation of neural crest progenitor cells into postmitotic sympathetic neurons [2]. Several agents have been established that induce neuroblastoma cell differentiation into neuron-like cells *in vitro*, such as retinoic acid and neurotrophins [3].

Earlier studies have defined certain signaling pathways downstream of neurotrophin receptors, involving Ras/MEK/ERK1/2 and PI3K/Akt activation and leading to execution of a signaling program that mediates cell cycle arrest or differentiation [4]. Crosstalk between cell surface receptors and signaling pathways is a hallmark of cell functioning through which cells interpret the environmental clues in normal and pathological conditions [5]. Both epidermal growth factor receptor (EGFR) and the urokinase-type plasminogen activator receptor (uPAR) produce signals that control cell proliferation and differentiation [6, 7].

EGFR is a member of the ERB tyrosine-kinase receptor family that interacts with a number of growth factors, including EGF, TGF-β and heparin-bound epidermal growth factor-like (HB-EGF) ligand [8]. Ligand binding induces receptor dimerization and phosphorylation/activation of the receptor tyrosine-kinase intracellular domain, which recruits and activates transducing elements of the Ras/ERK pathway leading to intracellular signaling responsible for cell proliferation, migration, survival, and differentiation [9]. In case of prolonged action, EGF causes internalization of EGFR, which abrogates the EGFR signaling cascade and abolishes EGF effects [10, 11]. Activation of EGFR in neurons is important for their survival: particularly, the neuroprotective effect of urokinase system in hippocampal ischemia is mediated through EGFR activation [12] and the loss of EGFR-dependent signaling in astrocytes of the cerebral cortex leads to their apoptosis and concomitant neuronal death [13].

uPAR is a multifunctional protein: besides its primary ligands, including urokinase and vitronectin, uPAR laterally interacts with integrins and growth factor receptors such as PDGFR

and EGFR [5, 14-17]. Also, uPAR expression ~~modulate~~ modulates TrkC expression [4]. uPAR interaction with growth factor receptors via integrins initiates a range of intracellular signaling including MAPK/ERK, JAK/STAT, SMAD, tyrosine kinase and serine kinases [6].

It is well-known that uPAR ~~has been shown to be~~ is involved in neuronal differentiation and morphogenesis of the nervous system in certain experimental models [18-20]. uPAR expression was detected in differentiating neurons from dorsal root ganglia [21]. In the developing central nervous system (CNS) uPAR is involved in the establishing of neural networks. Using chick embryonic optic tectum explant cultures, Lino and co-authors demonstrated that uPAR expression is spatially and temporally important for neuronal migration and neuritogenesis (E6-E12 embryonic stage) and subsequent synaptogenesis (E18-E21) [22]. Moreover, nerve growth factor (NGF)-driven neuronal differentiation of PC12 pheochromacytoma cells relies on uPAR expression since antisense oligonucleotides and uPAR blocking antibody inhibit the morphological and biochemical differentiation of these cells induced by NGF [18].

Under physiological conditions, uPAR expression is remarkably low, while uPAR is significantly upregulated during wound healing [23], inflammation [24] and cancer [25]. uPAR expression/secretion increases in tumor cells and/or in the surrounding stroma [26], which has been related to adverse patient outcomes in different types of cancer [26-40]. An intriguing aspect of uPAR functioning in cancer cells is that EGFR might serve as a downstream element in uPAR-mediated signaling as has been demonstrated for breast cancer and gastric carcinoma [14, 41]. Being among the most abundant growth factor receptors expressed in malignant tumors [9, 42], EGFR has been involved in a variety of cellular responses in neuroblastoma, such as proliferation and growth [43], differentiation [7], apoptosis [44] and chemoresistance [45].

~~In the present study we demonstrate that uPAR mediates proliferation, survival and differentiation of neuroblastoma Neuro2a cells. Serum withdrawal results in the formation of long neurites and is accompanied by increased expression of uPAR mRNA but not EGFR mRNA. uPAR overexpression causes increased EGFR phosphorylation. Blocking uPAR activity with antibody rapidly decreases EGFR (Y1068) phosphorylation and its downstream pERK1/2 (T202+Y204), but does increase Akt (S473), p38 (Y180/182) and c-Src (Y412) phosphorylation. Long-term uPAR blocking results in decreased survival and a loss of NeuN - neuron differentiation marker. EGF stimulates the rate of neurite growth (24 h) only in uPAR-overexpressing cells. Meanwhile, AG1478-mediated inhibition of EGFR activity impedes neurite growth in control cells and uPAR-deficient cells, but not in uPAR-overexpressing cells (24 h). Long-term EGFR blocking (120 h) results in the increased number of neurite-bearing cells in all cell types, however, in control and uPAR-overexpressing cells this effect is more~~

~~pronounced. Our results point towards a previously unrecognized role of uPAR as a regulator of EGFR activity in neuroblastoma cells, mediating their survival and differentiation.~~

In this paper we report our recent study of the mechanism of uPAR-mediated regulation of Neuro2a cell proliferation, survival and differentiation. Our data point towards a previously unrecognized role of uPAR as a regulator of EGFR activity in neuroblastoma cells.

Materials and methods

Cell culture

Mouse neuroblastoma cell line Neuro2a (ATCC® CCL-131™) was cultured in full growth medium containing DMEM (Hyclone) with high glucose, 10% FBS (Gibco), 1x MEM Non-Essential Amino Acids Solution (Gibco) and 1x Antibiotic-antimycotic solution (Gibco). Differentiation of Neuro2a was induced by serum deprivation using DMEM with 1% FBS for 24 h. To evaluate the effect of uPAR on cell proliferation, Neuro2a cells were seeded onto cell culture dishes at a concentration of 1×10^4 cells/well. To block uPAR function, cells were allowed to adhere and uPAR blocking antibodies (R&D, MAB531) (25 μg/ml) were added to the culture medium for 24 h. Cell number counting was carried out every 24 h for 120 h using automated cell counter Countess™ (Invitrogen).

Antibodies and reagents

The following primary antibodies were used: rat anti-uPAR (MAB531, RD Systems), rabbit anti-EGFR antibody (Ab2430-1), rabbit anti-pEGFR (#3777S), rabbit anti-ERK1 (pT202+pY204) + ERK2 (pT185 + pT187) (ab4819), rabbit anti-PARP-1 (sc7150), mouse anti-p38 (ab31828), rabbit anti-phospho p38 (pT180 + pY182) (ab32557), rabbit anti-c-Src, (sc18), rabbit anti-p-c-Src (sc101802). Secondary antibodies were AlexaFluor®488 or AlexaFluor®594 (Molecular Probes). Mouse anti-β3-tubulin (sc51670), rabbit anti-Histone H3 (#4499s) and rabbit anti-GAPDH (sc25778) antibodies were used in Western blotting experiments as protein loading control; HRP-conjugated donkey anti-rabbit IgG (Jackson Immuno-Research Laboratories) and HRP-conjugated anti-mouse IgG were used as a secondary antibody for Western blotting. Non-immune IgG in equivalent concentrations were used as a control.

Cell index measurement with automated IncuCyte® ZOOM analysis system

IncuCyte® ZOOM Live Cell Analysis System (Essen Bioscience) allows measurement of the changes in the cell confluence index in real-time, reflecting the changes in cell numbers in an automated mode. Neuro2a cells were plated in 12-well plates ($3x10^5$ cells/well) and placed in the IncuCyte® ZOOM system. The time-lapse imaging of 9 fields of vision in each well was carried out for 6 days with a frequency of every 2 h (as previously described) [46]. The curves reflecting the changes in the monolayer area over time were obtained using the IncuCyte® ZOOM image-processing software package. IncuCyte ZOOM's Confluence Processing Analysis tool allows the

calculation of the area covered by cells (mean percentage of the cell area in each well) using a cell-body cluster mask. Minimal cell size was limited to 350 mm^2 to exclude false-positive measuring of small cell fragments in the image.

Neuritogenesis Analysis

The impact of uPAR expression on neuritogenesis was performed using control Neuro2a cells (Neuro2a) or cells with different levels of uPAR expression (uPAR-deficient cells – Neuro2a-uPAR-KO; Neuro2a-uPAR – cells with uPAR overexpression). Neuritogenesis in Neuro2a cells was induced in low-serum conditions (DMEM with 1% FBS) and then evaluated in the presence of EGFR ligand – EGF (50 ng/ml) [47] or EGFR inhibitor AG1478 (20 μM) [48]; DMSO (0.2%) or BSA (50 ng/ml) were used as controls. Images were taken using a phase-contrast light microscope (Leica AF6000 LX) or an IncuCyte® system designed to study the neurite outgrowth and lengthening in real time.

The number of neurite-bearing cells was evaluated in randomly selected fields of view for 200 cells of each type using phase-contrast images.

Neurite length (mm/mm^2) was assessed using neurite mask of the IncuCyte® NeuroTrack Software Module algorithm (Cat No 9600-0010), which allows the automatic calculation of the average length of neurites and the normalization of them to the area occupied by the cell bodies. Cell images for this were taken every hour in 36-45 fields of view for each cell type during the next 5 days.

Cell lysates and Western blotting

Neuro2a cells were plated in full growth medium (DMEM with 10% FBS) onto 35 mm Petri dishes and were cultured overnight at 37°C in a CO_2 incubator. The next day, Neuro2a differentiation was induced by medium replacement. After the cells formed 70-80% cell monolayer, uPAR blocking antibodies (25 μg/ml) were applied for 5, 30, 120 min, 5 h or 24 h. For signal transduction assays, cells were treated with 100 μM AG1478 for 1 h or with vehicle (DMSO, 1%); or with 50 ng/ml EGF for 5 min or with BSA (50 ng/ml) as a control. AG1478 was dissolved in DMSO. Qproteome Cell Compartment Kit (QIAGEN) was used to segregate the proteins of different cell compartments. Cells were washed with cold PBS and lysed of lysis buffer (50 mM Tris-HCl, pH 8.0, 100 mM NaCl, 0.1 mM EDTA, 15 mM β-ME, 0.1 mM PMSF, 8% SDS, and 0.004% bromophenol blue and protease inhibitor cocktail 1:100).

Samples were electrophoresed in 10% SDS/polyacrylamide gel and electroblotted onto PVDF membrane (GE Healthcare). Kaleidoscope Prestained Standards (Bio-Rad Laboratories) were used as molecular weight markers. After rinsing in Tris-buffer saline (TBS: 150 mM NaCl, 50 mM Tris/HCl, pH 7.4), membranes were pre-blocked in TBSM buffer (TBS containing 5%

(w/v) of delipidated milk and 0.5% Tween 20) for 120 min. Membranes were incubated with primary antibodies for 24 h at 4°C, washed with TBSM, and then incubated with secondary antibodies conjugated with peroxidase for 1 h. Finally, membranes were washed in TBS containing 0.5% Tween 20 and visualized using SuperSignal West Pico Chemiluminescent Substrate (Thermo Scientific) and ChemiDoc™ XRS+ System (BioRad) for blot imaging and analysis.

Immunofluorescent staining and confocal imaging

Neuro2a cells were seeded onto the wells of a Nunc® Lab-Tek® Chamber Slide™ system at a low concentration ($2x10^4$/ml) in full growth medium; 24 h later the culture medium was changed for low serum medium (DMEM with 1% FBS). 24 h later, the slides were washed in HBSS, fixed with 4% formaldehyde, incubated with the first and the second antibodies and washed in HBSS. The nuclei were counterstained with DAPI. Images were acquired using a confocal laser scanning microscopy system (TCS SP5, Leica) equipped with 405 nm, 488 nm and 594 nm lasers. All images were captured with the same confocal gain and offset settings. The results of at least three independent experiments are presented. Qualitative analysis of the fluorescence intensity was calculated using ImageJ and corrected to the area of the selected cells and the mean fluorescence of the background (https://theolb.readthedocs.io/en/latest/imaging/measuring-cell-fluorescence-using-imagej.html).

***uPAR* knockout in Neuro2a cells**

To obtain Neuro2a cells with *uPAR* gene knockout we used CRISPR/Cas9 technique as described earlier [4]. ~~One of the three clones (#6) previously described was used for the current research.~~

Overexpression and downregulation of uPAR in Neuro2a cells

To suppress endogenous uPAR expression in Neuro2a cells we used a commercially available plasmid vector encoding shRNA (uPAR shRNA Plasmid, Santa Cruz, sc-36782-SH) [19]. For uPAR overexpression, uPAR cDNA was cloned into a phCMV1 vector (Addgene). cDNA encoding uPAR was obtained from Neuro2A cells using the following primers: cDNA-uPAR forward 5'-ACCATGGGACTCCCAAGGCGGC-3', cDNA-uPAR reverse 5'-TCAGGTCCAGAGGAGGACGCCCCATAG-3'. The sequence of the insert (cDNA encoding uPAR) was confirmed by Sanger's sequencing using following primers: seqPrimer1-forward 5'-GAGTGACGTAAGTACCGCCT-3', seqPrimer2-reverse 5'-AACACTGGAAGCCATTCGGT-3', seqPrimer3-forward 5'-TCCAGAGCACAGAAAGGAGC-3' (Evrogen). Cell transfection was performed using Lipofectamine 2000 (Life Technologies) according to the manufacturer's protocol. After transfection, cells were cultured for 8 weeks in full growth medium containing

selective antibiotic G418 (at a final concentration 400 μg/ml, Sigma-Aldrich). Changes in the uPAR expression were assessed using immunofluorescence staining.

Quantitative Real-Time Polymerase Chain Reaction analysis (RT-PCR)

The RNeasy® Mini Kit (Qiagen, Germany) was used for the extraction of total RNA from Neuro2a cells after the induction of differentiation at various time points (0, 24, 48, 72 h). For cDNA preparation 1 μg of total RNA was used. The cDNA synthesis was carried out using SuperScript® III First-Strand Synthesis SuperMix for qRT-PCR (Thermo Fisher Scientific). To select the specific sequence primer, Primer-BLAST software was applied followed by pre-validation of the primer specificity with OligoAnalyzer 3.1 (available online at https://eu.idtdna.com/calc/analyzer). Further primers for murine uPAR [19], EGFR and β-actin (used as housekeeping gene) were obtained from Evrogen (Russia): uPAR forward 5'-CGCCACAAACCTCTGCAAC-3', uPAR-reverse 5'-CTCTGTAGGATAGCGGCATTG-3', EGFR-forward 5'-CCCATGCGGAACTTACAGCAA-3', EGFR-reverse 5'-TTGGATCACATTTGGGGCAAC-3', β-actin-forward 5'-AGTGTGACGTTGACATCCGTA-3', β-actin-reverse 5'-GCCAGAGCAGTAATCTCCTTCT-3'. The thermal cycling program was 94˚C for 15 sec, 62˚C for 15 sec and 72˚C for 20 sec for 40 cycles. A relative transcript level of uPAR was calculated using the $2^{-\Delta\Delta Ct}$ method.

DNA Comet Assay

To evaluate the DNA damage, we used a Comet Assay (Cell Biolabs OxiSelect™). Neuro2a cells were seeded in full growth medium onto plastic Petri dishes (d = 35 mm) and allowed to adhere and proliferate overnight. The next day, Neuro2a differentiation was induced by medium replacement (DMEM with 1% FBS). After the cells formed 70-80% cell monolayer, uPAR blocking antibodies (25 μg/ml) were added to the culture medium. Non-immune IgG was used as a control in an equivalent concentration. Images were acquired by a Leica AP6000LX microscope. Quantitative analysis of DNA degradation was performed using ImageJ (OpenComet plugin).

Statistical analysis

Statistical analysis was performed using STATISTICA 10 for Windows software (Statsoft, Inc. 1984-2011) using one-way ANOVA function and Newman-Keuls, Tukey's or Dunkan's post hoc test for multiple comparisons or using Student's T-test for two-way comparisons. A value of $p<0.05$ was considered statistically significant.

Results

We have previously demonstrated the results of uPAR suppression in the chain of the events leading to a decline in Neuro2a cell proliferation, upregulated apoptosis, decreased neuritogenesis and enhanced neurite branching [4, 19]. EGFR is known to be involved in a

variety of cellular responses in neuroblastoma, ~~such as cell proliferation [43], differentiation [7, 43, 44] and apoptosis [44].~~. We have now investigated the potential link between uPAR expression and EGFR-mediated neuroblastoma cell survival and differentiation. First, we obtained Neuro2a cells with different levels of uPAR expression.

Neuro2a cells with different levels of uPAR expression

For uPAR overexpression ~~in Neuro2a,~~ plasmid transfection ~~was performed using uPAR cDNA coding plasmid~~ (phCMV1-uPAR) ~~and~~ followed by selection in a medium containing gentamicin (G418) was performed. To suppress uPAR expression, we carried out transfection with a commercial shRNA construct or implemented a CRISPR/Cas9-mediated *uPAR* gene knockout technique [4]. We confirmed the results of uPAR suppression/overexpression at the mRNA level using specific primers and real-time PCR (Fig. 1), as well as at the protein level using Western blotting [4].

Induced differentiation in Neuro2a results in the augmented expression of uPAR mRNA, but not of EGFR

Neuritogenesis was induced in Neuro2a cells by serum deprivation (DMEM 1% FBS) as reported previously [7]. The sustained deprivation for 72 h resulted in a significant induction of long neurite outgrowth (Fig. 2A) and was accompanied by an increase in uPAR mRNA content (Fig. 2B). These results suggest the involvement of uPAR in neuritogenesis (differentiation) of Neuro2a cells or their survival upon serum deprivation (Fig. 4E).

It has been previously demonstrated that high EGFR activity is linked to neural cell proliferation/differentiation and is essential for neuron survival [49]. Therefore, we further estimated the EGFR mRNA expression (Fig. 2C) and EGFR activation levels (Fig. 2D) upon serum deprivation. Although EGFR expression was almost unchanged, an obvious decrease in the EGFR phosphorylation level was detected after 24 h and 48 h of deprivation. These data suggest a downregulation of EGFR activity due to a decrease of growth factor concentration in a low-serum condition. The expression of NeuN – nuclear marker of mature neurons [50] was maintained at the same level, indicating the unchanged cell viability and preserved differentiation status of Neuro2a cells in long-term deprivation conditions (Fig. 2D). Interestingly, the basal level of pEGFR was sustained upon deprivation (24h and 48h), suggesting an important role of EGFR activity in maintaining the differentiation status of Neuro2a cells (Fig. 2D).

uPAR blocking reverses EGFR phosphorylation and reduces neuronal nuclear marker NeuN expression in differentiated Neuro2a cells

~~Cross-talk between signaling pathways in human carcinoma [14] and in human gastric cancer cells [51] has been demonstrated previously.~~ Our previously published data pointed to a

pivotal role of uPAR in neuritogenesis and neurite branching in Neuro2a cells [19]. Given that induction of differentiation in Neuro2a cells resulted in an upregulated uPAR but not EGFR mRNA expression (Fig. 2B, C), we further tested whether uPAR triggers signaling pathways involving EGFR and regulates Neuro2a cell differentiation into neurons.

We blocked uPAR activity using anti-uPAR antibody in culture of differentiated and undifferentiated Neuro2a cells (Fig. 3). uPAR blocking in differentiated cells led to almost complete dephosphorylation of EGFR already 5 min after the anti-uPAR antibody application (Fig. 3A, C). Notably, the expression of NeuN gradually decreased and was scarcely detectable 24 h later (Fig. 3A). For undifferentiated cells, there was also a tendency to a reduction in EGFR activation (pEGFR) and a decrease in NeuN content after 5 h incubation with anti-uPAR antibody (Fig. 3B, C). The lack of a statistically significant difference for undifferentiated cells probably reflects the abundance of growth factors in the full growth medium that flatten the inhibiting effect of anti-uPAR antibody. The obtained data suggest the involvement of uPAR in maintaining the differentiated state via modulating the EGFR activity upon long-term cultivation in low-serum conditions.

uPAR blocking causes increased activation of c-Src, Akt and p38 and a decline in ERK1/2 phosphorylation in Neuro2a differentiated

Next, we examined the effect of uPAR blocking antibody on EGFR-mediated signaling including ERK1/2, Akt, p38 and c-Src [51]. We detected a rapid decrease in phosphorylation of MAP kinase ERK1/2 after 5 min of uPAR blocking cells (Fig. 4A), an increase in Akt activation starting at 2 h and reaching its maximum at 5 h, and a gradual rise in phosphorylation of p38 and cytosolic Src-kinase starting at 2 h and reaching its maximum at 24 h (Fig. 4A).

uPAR protects differentiated Neuro2a cells from apoptosis

Prolonged exposure to uPAR-blocking antibody (120 h) resulted in a 3.7-fold decrease in the number of cells compared to control IgG (Fig. 4B). To gain further insight into the physiological role of uPAR, we analyzed the effect of uPAR blocking on the induction of apoptosis in differentiated Neuro2a cells. We tested the extent of PARP-1 cleavage (Poly (ADPribose) polymerase – PARP) in total protein extracts using Western blotting (Fig. 4A) and employed DNA-comet assay to evaluate cellular DNA damage (Fig. 4C-E). Caspase 3 cleaves PARP-1, the enzyme which normally participates in the DNA repair [52] during programmed cell death [53]. By 24 h, we detected a limited proteolysis of PARP-1 demonstrating apoptosis in Neuro2a cells (Fig. 4A).

The onset of DNA degradation in Neuro2a cells was registered by DNA-comet assay. Quantitative analysis of DNA degradation was performed using ImageJ (OpenComet plugin) [54]. The cell samples were electrophoresed to separate intact DNA from damaged fragments,

stained with a FITC-conjugated DNA dye and visualized by a Leica AP6000LX fluorescent microscope (Fig. 4C). Under these conditions, the damaged DNA migrated further than intact DNA and produced a "comet tail" shape (green fluorescence). The extent of DNA degradation level was estimated by the ratio of a comet tail length to the total fluorescence of an individual nucleus. Intact nuclei were marked by ImageJ plugin mask (red ovals and red numbers). After 72 h, uPAR blocking resulted in a 2.5-fold increase in the DNA degradation level compared to control cells (Fig. 4D).

Comets were evaluated by a tail length and later classified as previously described [55]. The method has been designed for visual evaluation of the DNA damage according to the percentage of DNA in a comet and allows the classification of the cells into 5 categories. The first category (None) included the intact Neuro2a cells or those with less than 5% of the DNA damage. The second (Low) contained cells with nuclear DNA fragmentation in the range from 5% to 25%. The third included cells with the DNA damage within 25-40% (Medium), the fourth – 40-95% of the DNA in a comet tail (High). The last category (Total) comprised the cells with more than 95% of the DNA damage [55]. Insignificant or minor DNA degradation was detected in both, control cell and cells incubated with anti-uPAR antibody, however, medium and high DNA damage was 10-fold and 5-fold higher in anti-uPAR antibody treated cells, respectively, suggesting an enhanced Neuro2a cell apoptosis (Fig. 4E).

Based on the aforementioned finding, we infer that uPAR plays an important role in Neuro2a cell survival and differentiation into neurons with the underlying possible mechanism being the activation of EGFR and its downstream effectors.

uPAR expression in Neuro2a cells affects pERK1/2 content in the cytoplasm via regulation of EGFR activity

To corroborate the specificity of the obtained results, the role of uPAR was further examined using an alternative approach. We assessed EGFR phosphorylation in cells with different levels of uPAR expression. Control (Neuro2a), uPAR-overexpressing cells (Neuro2a-uPAR) or cells with decreased uPAR (Neuro2a-sh-uPAR) (Fig. 5) were induced towards neuronal differentiation for 24 h, then fixed in non-permeabilizing conditions and double immunostained with antibodies against uPAR and pEGFR for confocal microscopy (Fig. 5A) and Western blotting (Fig. 5B). While the level of EGFR expression as detected by RT-PCR (Fig. 5C) and Western blotting remained unchanged in all cell types (Fig. 5B), uPAR overexpression resulted in augmented level of phosphorylated EGFR (Fig. 5B, D). Uncropped images of Western blots for Fig. 5B are presented in Supplementary Fig. 1. Immunofluorescent analysis with semiquantitative evaluation confirmed these results and demonstrated a tendency towards enhanced phosphorylation of EGFR in uPAR-overexpressing cells (Neuro2a-uPAR)

(Fig. 5A, E). Immunofluorescent staining of control Neuro2a cells, uPAR-overexpressing cells and a subpopulation of Neuro2a cells after CRISPR/Cas9n editing for uPAR knockout are presented in Supplementary Fig. 2.

To further elucidate the role of EGFR as a downstream effector of uPAR-induced signaling to ERK1/2, we examined whether administration of AG1478, ~~a highly potent and~~ (specific inhibitor of EGFR tyrosine kinase [56]), and EGF (EGFR ligand), affected ERK1/2 signaling and whether this signaling had a physiological function in Neuro2a cells.

Using cytoplasmic/nuclear fractions and Western blotting, we assessed pERK1/2 content in cells with different levels of uPAR expression (Fig. 6). In control conditions (DMSO was used as a solvent for AG1478) pERK1/2 (T202+Y204) content was relatively high in control (Neuro2a) and uPAR-overexpressing cells (Neuro2a-uPAR), however pERK1/2 was absent in Neuro2a-uPAR-KO cells. EGFR inhibition with AG1478 completely diminished pERK1/2 content in uPAR-expressing cells (Neuro2a and Neuro2a-uPAR cells), while in Neuro2a-uPAR-KO cells AG1478 induced increase in pERK1/2 content (Fig. 6A, B). In the nuclear fraction the content of pERK1/2 remained the same in all cell types upon AG1478 treatment (Fig. 6A, C).

It has been demonstrated that the presence of pERK1/2 in the cytoplasm is associated with EGFR activity resulting in pERK1/2-mediated cell signaling and cell differentiation [57, 58]. Overall, the AG1478 treatment resulted in the reduction of the cytoplasmic pERK1/2 in uPAR-expressing cells compared to control conditions (DMSO), pointing to the involvement of uPAR in the regulation of EGFR signaling and its downstream elements in the cytoplasm. The increase in pERK1/2 content in the cytoplasmic fraction of Neuro2a-uPAR-KO upon AG1478 treatment can reflect the overall altered signaling in Neuro2a-uPAR-KO cells. These data suggest the involvement of uPAR in the regulation of EGFR signaling and its downstream elements in the cytoplasm.

EGF-mediated EGFR activation in control and uPAR-overexpressing cells is accompanied by a reduction in pERK1/2, moreover, in Neuro2a-uPAR cells pERK1/2 content was below detection level. In contrast, in Neuro2a-uPAR-KO cells EGFR activation led to the increase in pERK1/2 content (Fig. 6D, E). Notably, pERK1/2 content in the nuclear fraction remained unchanged upon EGF treatment (Fig. 6D, F).

~~It is known that pERK1/2 intracellular localization could be responsible for activation of cell signaling resulting in both cell proliferation and apoptosis [60]. pERK1/2 signaling appears to be dependent upon the type of stimuli and the cell-specific context: translocation of the activated ERK1/2 into the nucleus correlates with cell proliferation, while cytoplasmic retention of pERK1/2 can result in inhibition of the survival/proliferation signals [60] or can be associated with cell differentiation [61] as has been shown for myogenic differentiation of the muscle~~

~~progenitor/stem cells [59].~~ Uncropped images of Western blots for Fig. 6 are presented in Supplementary Fig. 3.

Neurite growth rate is regulated by uPAR-mediated EGFR activation

Next, we compared the Neuro2a differentiation and proliferation using IncuCyte® *in vivo* assessment system of cell index (reflecting cell proliferation or enhanced cell size) and neurite length or neurite outgrowth (differentiation).

NeuroTrack (NT) processing module of the IncuCyte time-lapse microscopy system (IncuCyte® ZOOM Live Cell Analysis System, Essen Bioscience, USA) was applied as a tool to quantify the length of ~~neurites formed by Neuro2a cells with different levels of uPAR expression~~.neuritis. The cells were induced to differentiate in low-serum conditions and then AG1478 or EGF was added into the culture media. Real-time monitoring of neurite growth was performed within the next 36 h. Our results indicated that the increase in neurite length upon EGFR activation was detected only in cells overexpressing uPAR. In control conditions Neuro2a-uPAR cells formed the longest neurites (in DMSO or BSA). In contrast, in Neuro2a-uPAR-KO cells no neurite elongation was detected (Fig. 7A, C), which is in accordance with our previously published data demonstrating that suppression of uPAR activity with anti-uPAR antibody diminished the rate of neurite growth [19]. AG1478-mediated inhibition of EGFR activity impeded neurite growth in control cells and uPAR-deficient cells, but not in uPAR-overexpressing cells (Fig. 7B).

Activation of EGFR with EGF stimulated neurite growth rate in Neuro2a-uPAR cells (24 h) and the neurite length in those cells was 2-fold longer than in Neuro2a or Neuro2a-uPAR-KO cells ($p<0.05$) (Fig. 7D). After 36 h, the length of neurites was the same in control and uPAR-overexpressing cells. We surmise that uPAR protects Neuro2a cells from AG1478 effects, since particularly uPAR expressing cells maintained high neurite growth rate in the presence of the EGFR inhibitor. The effect of EGF the neurite growth rate was more pronounced in uPAR-expressing cells, further pointing to uPAR as playing an important functional role in EGFR-mediated Neuro2a cell neuritogenesis.

We also evaluated long-term (120 h) effects of AG1478 and EGF on neurite-bearing cells using ImageJ. The highest number of neurite-bearing cells was always detected in uPAR-expressing cell cultures (control Neuro2a and Neuro2a-uPAR) and the number of neurite-bearing cells in Neuro2a-uPAR-KO cultures was the lowest regardless of the presence or absence of AG1478/DMSO or EGF/BSA (Fig. 7E). Upon EGF or BSA administration, the number of neurite-bearing cells in Neuro2a-uPAR cultures was always 30% higher ($p<0.01$) than in Neuro2a cells. Surprisingly, AG1478 significantly stimulated neurite formation in all three cell types, which can be attributed to the previously described non-canonical side effects of AG1478

to stimulate p75(NTR) receptor proteolysis [59]. Unexpectedly, in DMSO conditions there was a slightly higher number of neurite-bearing cells in Neuro2a than in Neuro2a-uPAR cells (Fig. 7E).

Next, we compared the cell index of Neuro2a cells with different levels of uPAR expression using IncuCyte® system and cell-body cluster mask, which allow to evaluate the actual cell body area in a cell culture and can reflect cell proliferation. Cells were plated in DMEM with 1% FBS; EGF or BSA was immediately added to each well. EGF administration exerted no statistically significant effect on Neuro2a cell index (Fig. 8). There was only a tendency towards cell index increase in Neuro2a-uPAR-KO cells in the presence of EGF compared with BSA. The highest cell index throughout the experiment was detected in Neuro2a-uPAR cells irrespective of EGF or BSA administration. At 120 h, a statistically significant difference was detected between Neuro2a-uPAR cells versus Neuro2a and Neuro2a-uPAR-KO ($p<0.01$). The lowest cell index detected in Neuro2a-uPAR-KO cells in control conditions (BSA) probably reflects their impaired proliferation or survival, underscoring the important role of uPAR in these processes [4].

~~Thus, the data obtained show the relationship between uPAR and EGFR in the regulation of the EGFR-dependent pathway that involves ERK1/2 kinase that regulates cell proliferation and differentiation.~~

Discussion

Certain cell types such as glioma [60], neuronal stem cells [61] and neuroblastoma cell lines [7] undergo differentiation after serum withdrawal. Our initial analysis based on RT-PCR and Western blotting revealed that serum withdrawal had similar effects on cell differentiation and signaling mechanisms in Neuro2a cells as in the other well-established models. Serum deprivation stimulated differentiation/neuritogenesis (Fig. 2). Long-term serum deprivation of cultured neurons has been demonstrated to result in either differentiation or death [7, 62]. In the present study long-term serum withdrawal had no effect on cell survival (Fig. 4A) or differentiation status of neuroblastoma cells (Fig. 2D), but as expected, induced neuritogenesis. Interestingly, this was accompanied by increased expression of uPAR mRNA, but not EGFR mRNA, suggesting uPAR involvement in neuroblastoma differentiation (Fig. 2). ~~Despite serum withdrawal, EGFR activation was preserved in Neuro2a cells, while the total protein EGFR expression level remained unchanged (Fig. 2).~~

~~Surprisingly, blocking~~ Blocking the uPAR activity with specific antibody rapidly decreased phosphorylation of EGFR (Y1068) and its downstream ERK1/2 (T202+Y204), while long-term uPAR blocking (24 h) increased phosphorylation of c-Src (Y412), Akt (S473) and p38 (Y180/182) in Neuro2a cells (Fig. 3, 4). These data are in accordance with previously published

results ~~where it was demonstrated~~ indicating that ~~the~~ EGFR activation ~~of EGFR was~~ is necessary for Akt and ERK1/2 phosphorylation, while inhibition of EGFR, PI3K, ERK1/2 ~~blocked~~ blocks Neuro2a cell differentiation [7]. Differentiation of Neuro2a cells was induced in low serum conditions (1% FBS), therefore, the decrease in pEGFR from 0 to 24 h can be attributed to an overall decrease in growth factors in the culture medium, including EGF, which is normally present in FBS. Despite serum withdrawal, EGFR activation was preserved in Neuro2a cells (between 24 and 48 h), while the total protein EGFR expression level remained unchanged (Fig. 2). ERK and PI3K/Akt activation and their downstream signaling is known to regulate neuronal differentiation [63] and to protect neurons against drug-induced injury [64, 65]. In the PC12 cells (a well-established model to study cell differentiation and neuritogenesis), ERK1/2 is an important mediator of NGF-induced neurite outgrowth ~~in the PC12 cells~~, since MAPK inhibitors block neuronal differentiation in these cells [66]. α-lipoic acid, a well-known activator of PI3K/Akt signaling in neurons, requires pERK1/2 to mediate its effect on Neuro2a cell differentiation, since ERK1/2 inhibitor abolishes the α-lipoic acid effect on neurite outgrowth [67]. Placing EGFR downstream of uPAR, our results identify EGFR as a mediator of signals initiated by uPAR to ERK1/2, c-Src and Akt, which is in line with the previously published data ~~on other cancer cell lines~~ [14, 41, 68]. Genias and co-authors demonstrated that in MB-231 breast cancer cells and in MEFs, EGF administration resulted in EGFR tyrosine phosphorylation and ERK/MAP kinase activation mediated by STAT5 and accompanied by incremented mitogenic activity. The application of antibodies that block uPA binding to uPAR led to the decrease in ERK1/2 phosphorylation and the onset of apoptosis [69].

~~In the present study we demonstrated that the EGFR-ERK1/2 signaling pathway in Neuro2 cells was regulated by the expression and activity of uPAR. Anti-uPAR antibody that blocks uPAR activity reduced pERK1/2 (Fig. 4E), but led to enhanced formation of new neurites (i.e. the increased number of neurite-bearing cells) [19]. Suppression of EGFR-ERK1/2 signaling pathway was detected upon uPAR blocking with antibody (Fig. 3A, 4E) as well as in uPAR-deficient cells (Fig. 6D), which was followed by a decreased survival as demonstrated in Fig. 4 and in our previously published paper [4]. Therefore, we speculate that uPAR expression and activity is fundamental for the maintenance of EGFR-ERK1/2 activation, inrease in cell index (Fig.8) and regulation of cell differentiation (Fig.7).~~

~~Long-term uPAR blocking (72 h) resulted in the induction of pro-apoptotic cell signaling and cell death (Fig.~~ The observed effect of increased c-Src and Akt signaling can be a compensatory response, such as, the uPA/uPAR signaling initially inhibited by the blocking antibody within the first 2 h can be upregulated after 24 h (Fig. 4). Alternatively, uPAR can be activated by endogenously produced urokinase and can transmit signals to downstream c-Src and

Akt [25]. Whether Src activation results in apoptosis or cell survival depends on the c-Src targets – Akt and/or p38 [70, 71]. Since incubation with uPAR-blocking antibody for 72 h results in cell death, we surmise that 24 h c-Src activation transmits a pro-apoptotic signal, rather than a survival. Indeed, prolonged uPAR blocking resulted in the loss of neuron differentiation marker NeuN expression (Fig. 3A), reduced cell number (Fig. 4B),~~AG1478-induced suppression of EGFR-ERK1/2 signaling axis (within 120 h) led to an increase in the number of neurite-bearing cells in all cell types (Neuro2a, Neuro2a-Neuro2a-uPAR and Neuro2a-uPAR-KO) (Fig. 7E), however, in uPAR-deficient cells (Neuro2a-uPAR-KO) the number was significantly lower than in uPAR-overexpressing or control cells (Neuro2a-uPAR and Neuro2a). The most relevant explanation for this paradox is that ERK1/2 activation is essential for neurite elongation rather than for the formation of new neurites.~~

~~Prolonged uPAR blocking resulted in the loss of neuron differentiation marker NeuN expression, reduced proliferation,~~ induction of pro-apoptotic cell signaling, DNA damage and decreased survival (Fig. 3, 4). Earlier it has been established that the loss of NeuN is associated with various types of neuronal damage [72, 73]. PARP-1 cleavage fragment (89 kDa), revealed as a marker of apoptosis (Fig. 4A), is generally detected upon neurodegeneration [74] and neurological diseases accompanied by neuronal death, such as cerebral ischemia, Alzheimer's disease, multiple sclerosis, Parkinson's disease, craniocerebral trauma caused by NMDA excitotoxicity and brain tumors, especially glioma [75-77]. Using dorsal root ganglia 3D explant model, we have demonstrated earlier that uPAR blocking with this antibody resulted in the loss of radial axon growth, while in neuroblastoma cells it was manifested morphologically in the enhanced neurite branching [19]. Collectively these results indicate that uPAR functioning is indispensable for Neuro2a cell survival and maintaining the differentiated status.

To gain insight into the mechanisms of uPAR signaling effects and cellular changes in Neuro2a cells, we used uPAR overexpression/suppression approach (Fig. 1, 5-8). Indeed, uPAR overexpression led to the increase in EGFR phosphorylation (Fig. 5A) with no change in EGFR mRNA (Fig. 5C). In control settings (BSA), pERK1/2 was almost absent in the cytoplasmic fraction of Neuro2a-uPAR-KO cells, while in uPAR-expressing cells (Neuro2a and Neuro2a-uPAR cells) the cytoplasmic pERK1/2 was upregulated (Fig. 6 D, E). In these conditions (Fig. 7C) the rate of neurite growth in uPAR-expressing cells was higher than in Neuro2a-uPAR-KO cells, suggesting a correlation between uPAR expression and increased pERK1/2 content in the cytoplasm.

Unexpectedly, in response to EGF the content of activated ERK1/2 in the cytoplasm of uPAR-expressing cells (Neuro2a and Neuro2a-uPAR cells) decreased, while in Neuro2a-uPAR-KO cells pERK1/2 was upregulated (Fig. 6 D, E). ~~It is known that EGF binding to EGFR can~~

~~result in~~ A likely explanation for this is a uPAR-initiated interactome assembly on the cell membrane [5] and EGFR transactivation that may result in a rapid clathrin-dependent internalization of EGFR alone or as a part of the complex (EGF/EGFR/uPAR). We believe that such EGFR internalization with the subsequent degradation in the lysosomes ensuing suppression of EGFR-dependent signaling ~~[78]. We speculate that an enhanced EGFR internalization from the cell membrane upon EGF treatment can account for the observed decrease in the cytoplasmic pERK1/2 in uPAR-expressing cells. EGF administration stimulated neuritogenesis only in uPAR-expressing cells (control Neuro2a and Neuro2a-uPAR); specifically, Neuro2a-uPAR cells responded to EGF treatment 12 h earlier than control Neuro2a cells, while uPAR-deficient cells were insensitive to EGF administration (Fig.~~ may account for the decrease in pERK1/2 reported in the present study (Fig. 6D). Similar mechanism of EGFR internalization has been previously described for EGF-mediated long-term activation of EGFR, which abrogates the EGFR signaling cascade and EGF action [11].~~However, EGF-mediated activation of EGFR-ERK1/2 signaling pathway was not sufficient for neurite growth induction in Neuro2a-uPAR-KO cells (Fig. 7D, E).~~

ERK is known to be chiefly cytoplasmic in resting cells, but its activation/phosphorylation can result in the nuclear accumulation or cytoplasmic retention, where its function is essential for cell fate decision such as proliferation or differentiation [57]. Earlier studies indicate that in G_0-arrested fibroblasts ERK1/2 is mainly located in the cytoplasm, while upon stimulation by serum or mitogenic factors pERK1/2 is rapidly translocated into the nucleus where its access to transcription targets mediates cell proliferation response [79]. Retinoic acid–induced differentiation of F9 embryonic carcinoma and embryonic pluripotent stem cells is accompanied by restricted nuclear access of pERK1/2 resulting in reduced proliferation due to actin- and microtubule-dependent cytoplasm retention of pERK1/2 [80]. pERK1/2 shuttling between the nucleus and the cytoplasm was shown to function as a switch-like transition between proliferation and myogenic differentiation of muscle progenitors, respectively [58]. Our obtained results are in accordance with these published data and indicate that *uPAR* gene knockout resulted in reduction of cytoplasmic pERK1/2 content and in downregulation of Neuro2a differentiation, while uPAR overexpression, on the contrary, led to increased cytoplasmic pERK1/2 and neuritogenesis (Fig. 6, 7, 9). Compartmentalization of activated ERK1/2 at the plasma membrane or vesicular cell organelles or cytoskeleton can retain pERK1/2 in the cytoplasm and restrict nuclear entry [57]. Therefore, we speculate that unchanged pERK1/2 content in the nucleus detected in all cell types (Neuro2a, Neuro2a-uPAR-KO and Neuro2a-uPAR cells) may reflect retention of activated ERK1/2 in the cytoplasm. In addition, we have previously shown that uPAR overexpression alone in Neuro2a cells results in

ERK1/2 activation and its complete translocation into the nucleus, where it is presumably involved in the regulation of gene expression responsible for cell proliferation and/or epithelial-mesenchymal transition (EMT) [46].

In the current paper we detected the stimulating effect of EGF on neuritogenesis only in uPAR-expressing cells underpinning the role of uPAR in EGFR-mediated cell signaling and neurite growth (Fig. 7). EGF administration stimulated neuritogenesis in control Neuro2a and Neuro2a-uPAR cells; specifically, Neuro2a-uPAR cells responded to EGF treatment 12 h earlier than control Neuro2a cells ($p < 0.05$), while Neuro2a-uPAR-KO cells were insensitive to EGF administration (Fig. 7D, E). Therefore, in the absence of uPAR Neuro2a cells do not respond to EGF resulting in impaired differentiation and significantly attenuated neurite growth (Fig. 7E).

AG1478, a specific EGF receptor kinase inhibitor [56], was shown to block uPAR-induced ERK1/2 phosphorylation in human carcinoma cells, suggesting that EGFR serves as an adapter protein in the molecular pathway that combines uPAR activation with ERK1/2 phosphorylation in these cells [14]. Along with these data, we demonstrate that in uPAR-expressing cells (Neuro2a and Neuro2a-uPAR), AG1478 administration resulted in the reduction of pERK1/2 content in the cytoplasm (Fig. 6 A, B). Surprisingly, AG1478-induced suppression of EGFR/ERK1/2 signaling axis (within 12 h) led to an increase in ~~uPAR-overexpressing~~ the number of neurite-bearing ~~cells AG1478 treatment enhanced~~ in all cell types (Neuro2a, Neuro2a Neuro2a-uPAR and Neuro2a-uPAR KO) (Fig. 7 B, E), however, in uPAR-deficient cells this number was significantly lower than in uPAR-expressing cells. One of the possible explanations can be that ERK1/2 activation is essential for neurite elongation rather than for initiation of new neurites. The "off-target effect" of AG1478 resulting in enhanced neuritogenesis due to the AG1478-induced release of neurotrophins in retinal ganglion cell culture and neurotrophin-induced intramembranous proteolysis of p75(NTR) has been described earlier by Douglas et al. [59]. Our data are in accordance with these results. AG1478 stimulating effect on neuritogenesis can be attributed to the previously described non-canonical side effect of AG1478 on p75(NTR) receptor proteolysis. Earlier we have published results demonstrating a tendency to decrease the level of p75(NTR) expression in uPAR-deficient Neuro2a cells [4], which may account for a more pronounced effect of AG1478 in these cells compared to uPAR-expressing cells (Fig. 7). Interestingly, in CHO-K1 cells that do not express EGFR, ERK1/2 can be activated in response to uPA treatment underlying the existence of alternative EGFR-independent pathways involving uPAR. This response was insensitive to AG1478 [81].

To test a hypothesis if the increase in cell differentiation/neuritogenesis in the presence of AG1478 correlates with AG1478-mediated inhibition of the mitogenic function of EGFR rather than of EGFR effect on neurite growth assessed cell index using the IncuCyte® system

(Supplementary Fig. 4). Previously, we have demonstrated that uPAR-overexpressing cells exhibit enhanced proliferation, as evaluated by Ki-67 expression (a marker of proliferating cells) [46], while *uPAR* knockout cells display a dramatic phenotypic change – an increase in the cell body size and epithelial to mesenchymal transition (EMT) [46]. After AG1478 treatment for 120 h, the cell index was decreased in all cell types (Neuro2a, Neuro2a-uPAR, and Neuro2a-uPAR-KO) compared to DMSO (Supplementary Fig. 4). However, the most drastic effect was observed in Neuro2a-uPAR-KO cells – 3.9-fold decrease ($p < 0.0001$), in Neuro2a-uPAR cells – 2.4-fold decrease ($p < 0.0001$) and in Neuro2a cells – 1,6-fold decrease ($p < 0.01$) (Supplementary Fig. 4). Therefore, by 120 h the increased cell index in the presence of DMSO in Neuro2a-uPAR cells can be attributed to upregulated cell proliferation, while in Neuro2a-uPAR-KO cells elevated cell index may be related to the increased cell size and phenotypic change. Recently, we described a novel mechanism of urokinase functioning in Neuro2a cells [46] in the absence of uPAR, uPA is translocated into the nucleus where it is involved in the activation of transcription factors (NF-kβ and Snail) resulting in endothelial to mesenchymal transition (EMT) [46].

Combining the results obtained in the present study with our previously published data, we infer that uPA/uPAR system has a significant impact on Neuro2a cell morphology. As reported earlier, blocking the uPA/uPAR interaction with antibody causes neurite branching, but does not affect the rate of neurite growth [19]. It appears that uPAR expression stimulates elongation of existing neurites, since uPAR-expressing cells (control Neuro2a or uPAR-overexpressing cells) regardless of the presence or absence of AG1478/DMSO or EGF/BSA always demonstrate an increase in neurite length compared to uPAR-KO cells (Fig. 7). Therefore, summarizing our current data (Fig.9) and previously published results [19] we conclude that uPA/uPAR and EGFR signaling (Fig. 6) play a pivotal role in Neuro2a differentiation/neuritogenesis.

~~This response was insensitive to AG1478 [82]. It has been revealed in earlier studies that different ligands can define EGFR dimerization strength and signaling dynamics and can influence cellular response [8].~~

~~Thus, varying cellular responses can be evoked depending on whether EGFR is either transactivated by uPAR in cells that express uPAR or is activated by EGF, its own ligand in uPAR-deficient cells, revealing the complex integrated interactions of the cell surface receptors and modulation of EGFR control system by uPAR. We infer that our data suggest that uPAR regulates EGFR activity and its downstream signaling to ERK1/2, potentially implicating uPAR in the regulation of ERK1/2 cytoplasmic targets that regulate the rate of neurite growth.~~

Conclusion

Our data lead us to a conclusion that uPAR is an important regulator of neuroblastoma cell survival and differentiation. uPAR overexpression results in enhanced cell index, potentially reflecting cell proliferation. uPAR can influence the state of phosphorylation and signaling activity of EGFR, thus affecting the activation status of ERK1/2, the primary EGFR downstream target. uPAR is upstream of the EGFR/ERK1/2 signaling pathway, and the latter controls cell survival in the absence of uPAR and promoting neurite growth in uPAR-expressing cells. These findings demonstrate a molecular pathway linking uPAR with EGFR/ERK1/2 signaling in governing Neuro2a cell proliferation, differentiation and apoptosis, representing uPAR as a rational target molecule for manipulating neuroblastoma (Fig. 9).

EGFR is upregulated or aberrantly activated in many cancer types. Since EGFR was detected to be downstream of uPAR, blocking the uPAR activity or manipulating *uPAR* gene expression might be an excellent target for anticancer therapy [4, 82-86].

Funding

This research was supported by the Russian Science Foundation (project number 19-75-30007) and RFBR (project number 20-015-00186). CRISPR/Cas9 *PLAUR* downregulation and uPAR overexpression experiments using Neuro2a cells were supported by Grant № 20-015-00186 and the rest was supported by RSF project №19-75-30007. This study was conducted using biomaterial collected within the frame of Moscow University Project "Noah's Ark" and equipment purchased as a part of Moscow State University Program of Development.

Authors' contributions

Rysenkova and Semina designed the experiments, performed data acquisition and analyzed the obtained results; Klimovich, Shmakova, Karagyaur, Alexandrushkina and Ivanova performed data acquisition and statistical analysis; Rubina and Semina contributed to the discussion of the obtained results, Rubina contributed to the manuscript writing; Tkachuk made a substantial contribution to the main concept of the manuscript. All authors have read and approved the final version of the manuscript.

Figures

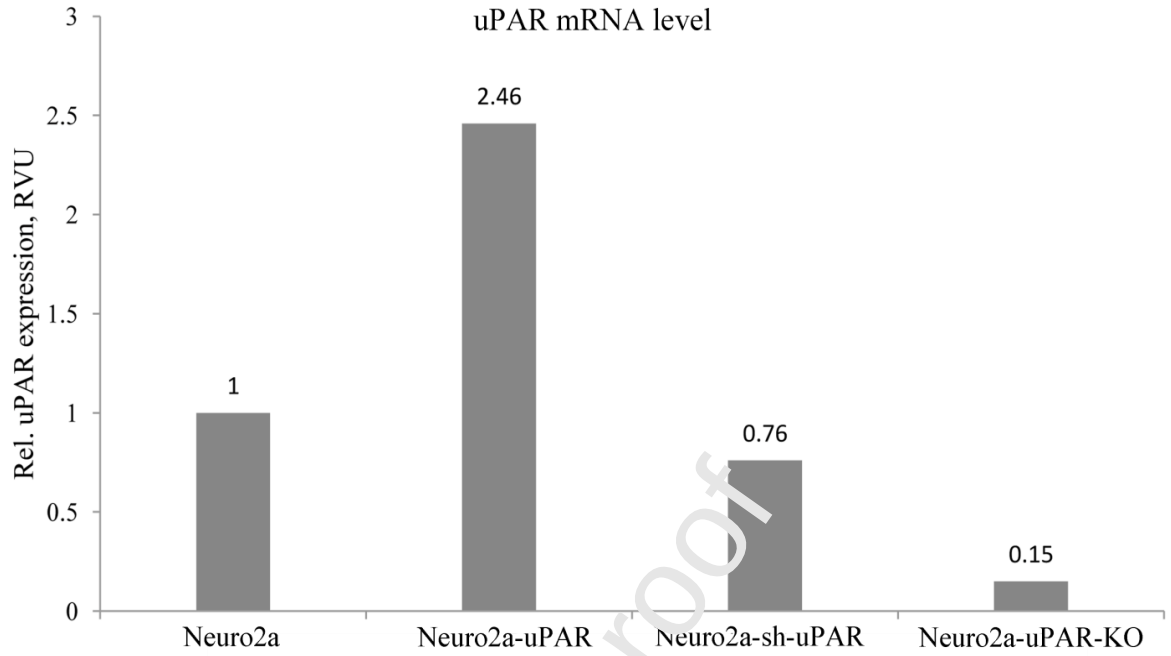

Fig. 1. uPAR expression level evaluated using RT-PCR analysis in Neuro2a cells. Neuro2a – control cells; Neuro2a-uPAR – uPAR-overexpressing cells obtained by cell transfection with phCMV1-uPAR plasmid and subsequent selection using G418; Neuro2a-sh-uPAR – Neuro2a cells with downregulated uPAR expression using shRNA; Neuro2a-uPAR-KO – Neuro2a cells with *uPAR* knockout. The reproducible result of one of three independent experiments is presented (N=3).

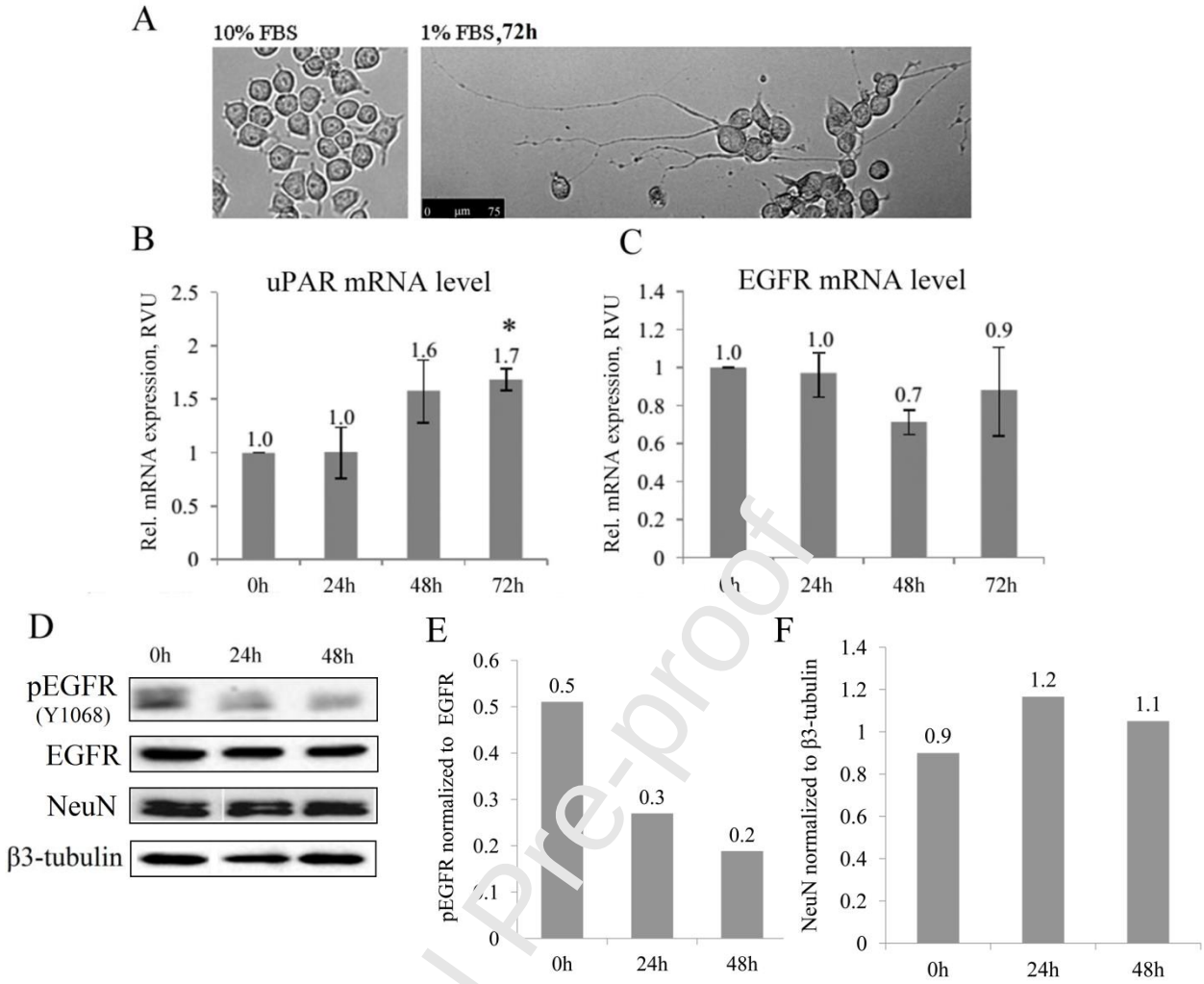

Fig. 2. Serum deprivation in Neuro2a cells resulted in upregulated uPAR mRNA level, while the expression level of EGFR mRNA and pEGFR stayed unchanged. A – Neuro2a possess long neurites upon 72h of serum deprivation (1% FBS) (N=30). Scale bar 75 μm; B – uPAR mRNA expression level evaluated using RT-PCR analysis in Neuro2a cells after 24h, 48h, 72 h of serum deprivation, *p<0.05 (by ANOVA, Dunkan's test); C – EGFR mRNA expression level evaluated using RT-PCR analysis in Neuro2a cells after 24 h, 48 h, 72 h of serum deprivation; data are presented as mean values of +/- SEM (N=3). D – Western blotting analysis of EGFR, pEGFR, and NeuN in Neuro2a cells (N=2). E, F – a densitometry analysis of the results. β3-tubulin was used as the loading control. ~~Scale bar 75 μm.~~

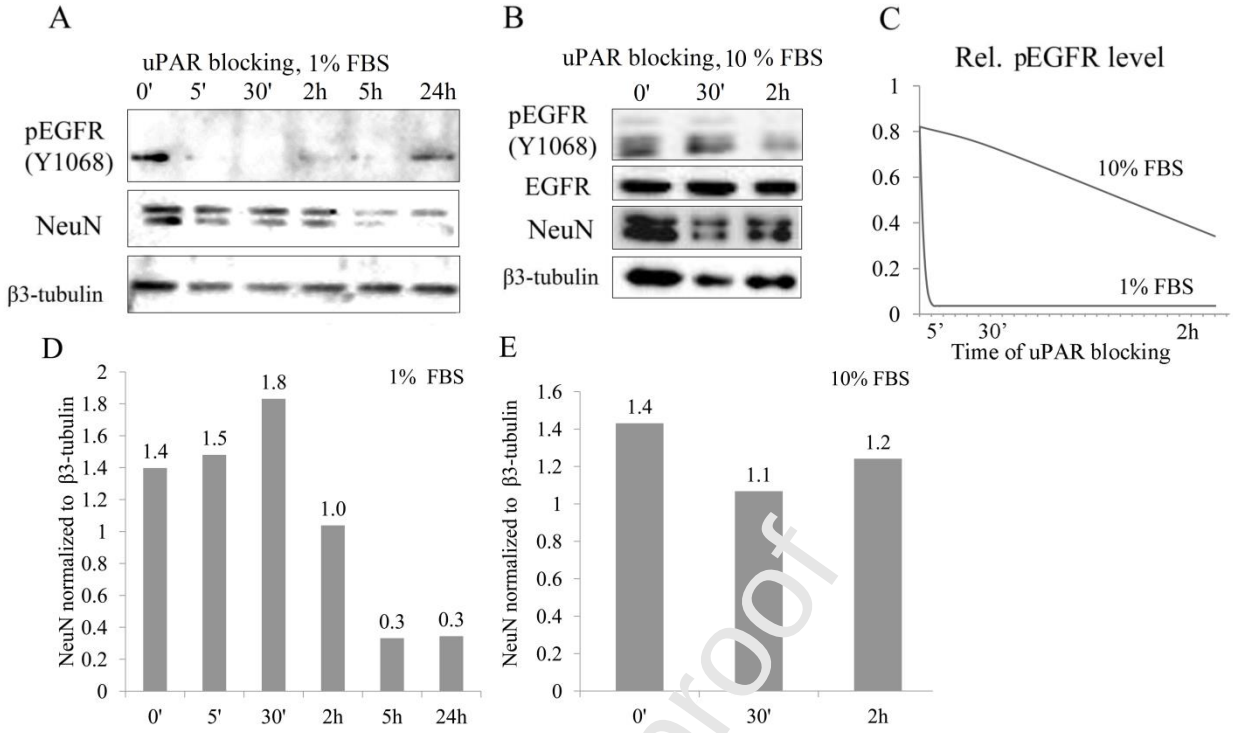

Fig. 3. Blocking uPAR in Neuro2a decreased the level of neuron markers such as NeuN and pEGFR phosphorylation. Blocking of uPAR activity was performed using blocking antibodies at a concentration of 25 µg/ml. A – analysis of pEGFR and NeuN levels in serum deprivation conditions (1% FBS) after 5 min, 30 min, 2 h, 5 h, 24 h (N=3); B – analysis of the content of pEGFR and NeuN in a full-fledged culture medium (10% FBS) after 5 min, 30 min, 2 h, 5 h, 24 h (N=2); C – a densitometry analysis of the pEGFR content ~~in shrinkage due to~~ ; D, E – a densitometry analysis of the NeuN content.

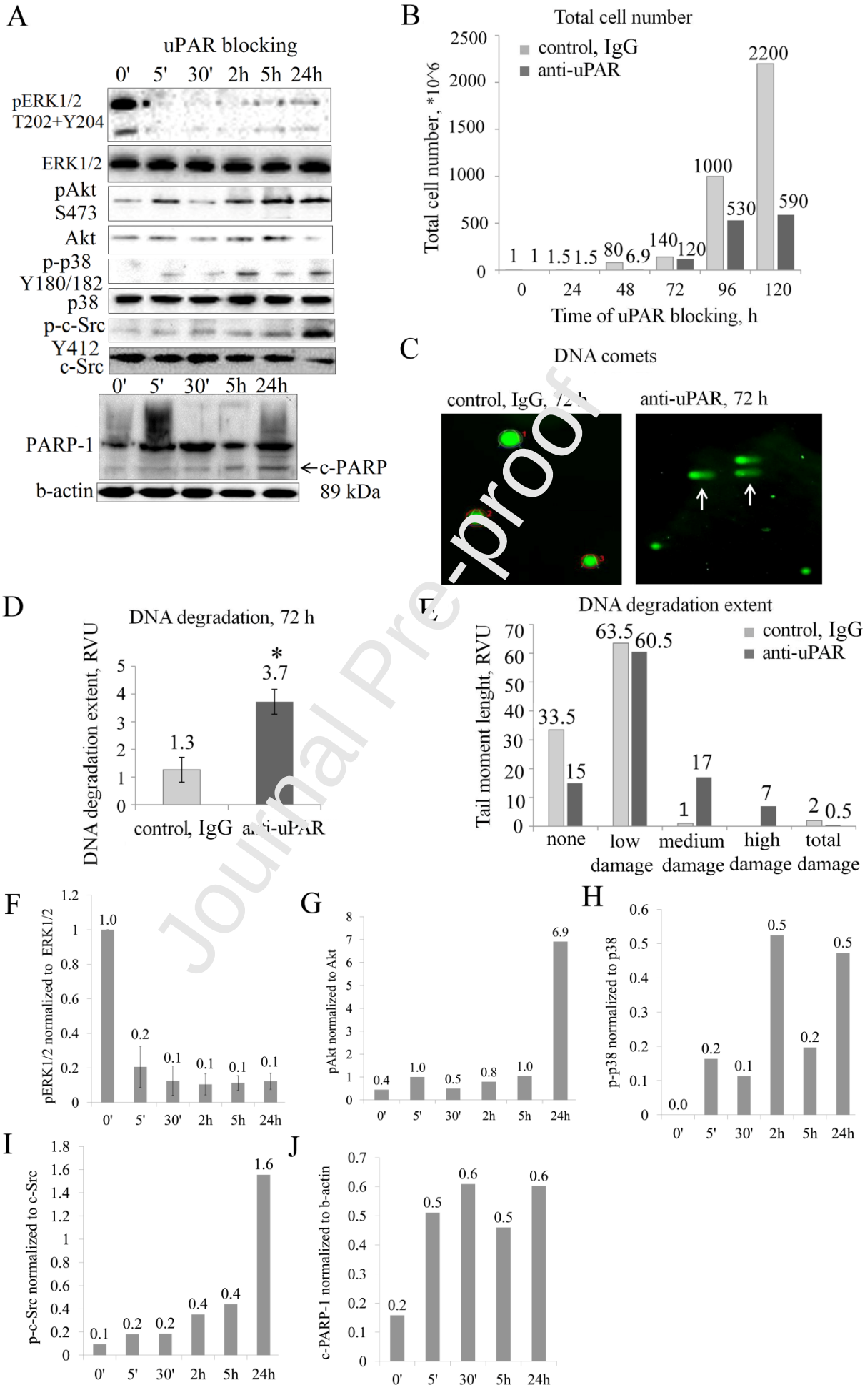

Fig. 4. uPAR blocking in Neuro2a cells decreased the total cell number, which was accompanied by the induction of pro-apoptotic cell signaling with ERK1/2, Akt, p38 and c-Src, PARP-1 proteolysis and DNA degradation. A – Western blotting analysis of the level of pERK1/2, pAkt, p-p38, p-c-Src and PARP-1 upon uPAR blocking; b-actin was used as a loading control (N=3). B – total cell number was calculated using automated cell counter Countess™, anti-uPAR – using uPAR-blocking antibodies or IgG as a control. C – microscopy photograph of agarose gel with nuclei of Neuro2a cells stained with FITC. After incubation of Neuro2a in the presence of antibodies, blocking uPAR at a concentration of 25 μg/ml for 72 h, electrophoresis under alkaline conditions (method DNA comets) (N=5). Rat IgG was used as a control. Arrow points out the cells with increased DNA degradation that form a comet-like shape of nuclei (green). The intact nuclei in control conditions are encircled in red ovals and marked by red numbers. D – quantitative analysis of DNA degradation was performed using ImageJ (OpenComet plugin), *$p<0.05$. E – assessment of the degree of DNA degradation. F-J – a densitometry analysis of the ~~Western blotting analysis of the level of pERK1/2, pAkt, p-p38, p-c-Src and PARP-1 upon uPAR blocking. -actin was used as a loading control~~results.

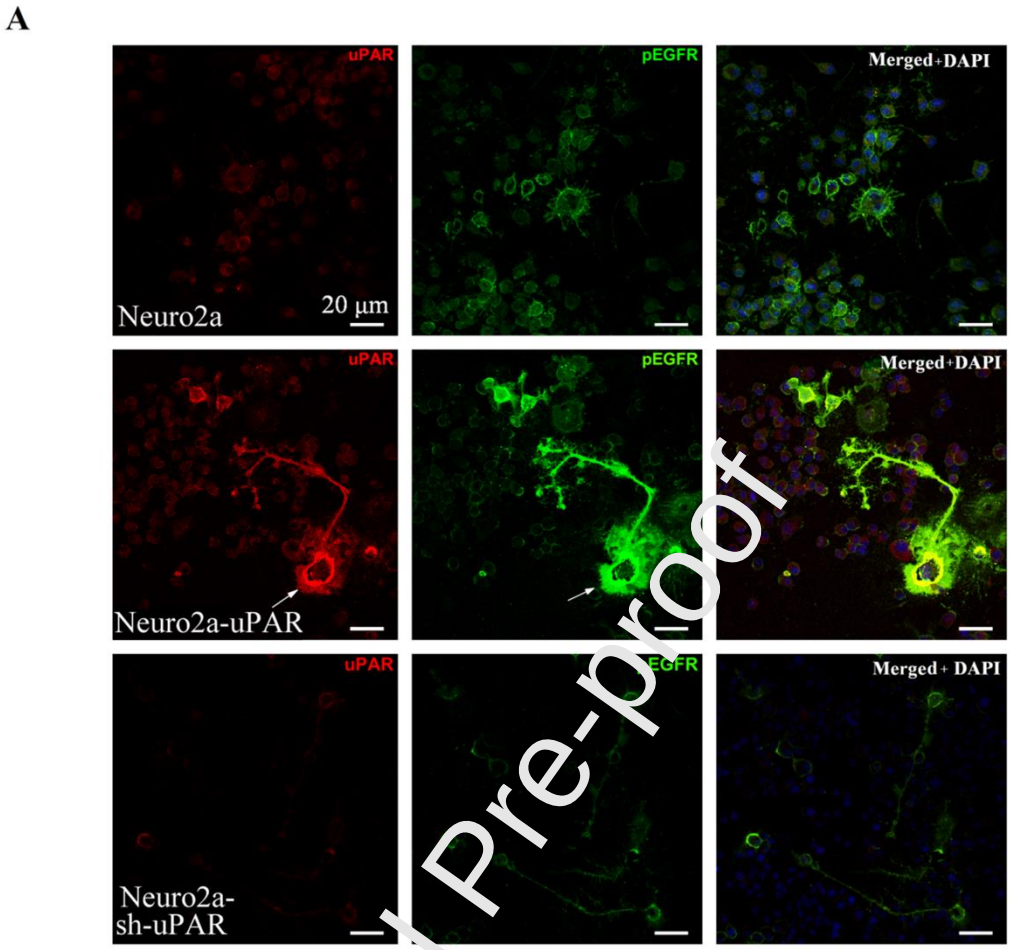

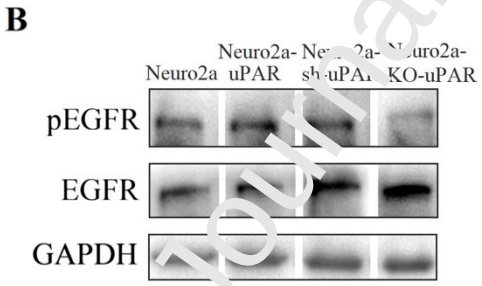

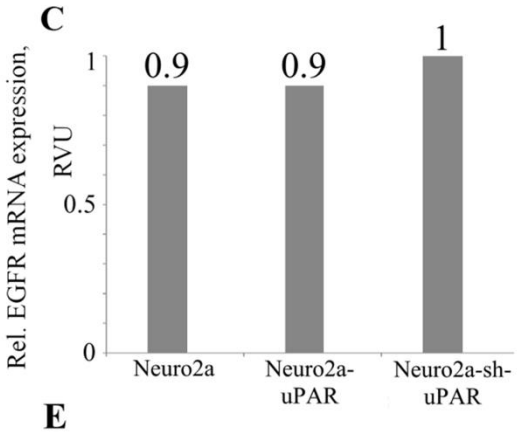

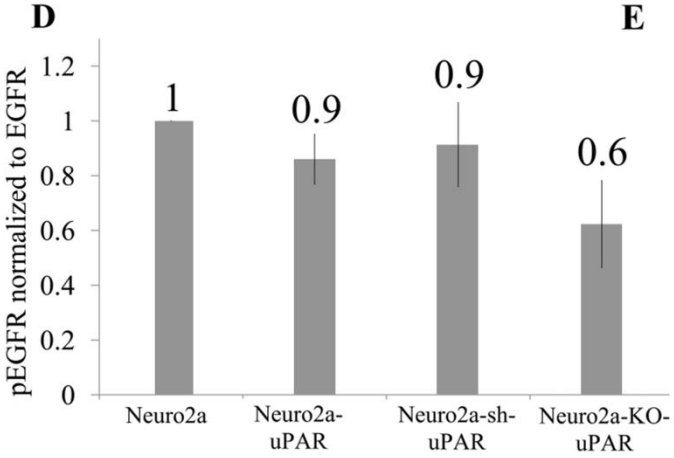

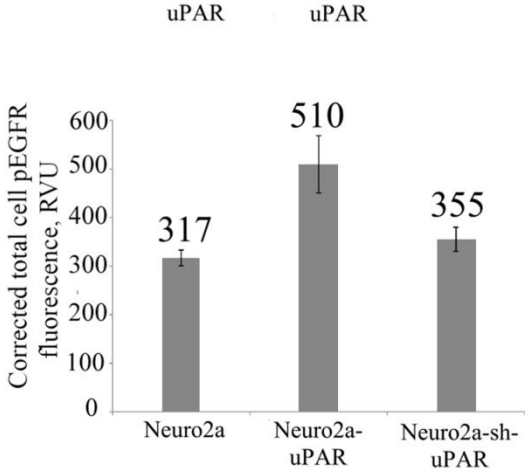

Fig. 5. uPAR overexpression stimulates EGFR phosphorylation in Neuro2a cells. A – immunofluorescent staining with anti-uPAR (red fluorescence) and anti-pEGFR (green fluorescence) in control Neuro2a cells (Neuro2a), Neuro2a cells with uPAR overexpression (Neuro2a-uPAR) or Neuro2a cells with uPAR downregulation (Neuro2a-sh-uPAR). Nuclei are counterstained with DAPI. Arrow points out a cell with increased expression of uPAR, in which also an increase in phosphorylation EGFR occurs. Scale bar 20 μm. B – Western blot analysis of total EGFR and pEGFR levels, GAPDH was used as the loading control (N=3). C – EGFR mRNA expression level evaluated using RT-PCR in Neuro2a cells with different uPAR levels; D – a densitometry analysis of the results. E –The corrected total cell fluorescence (CTCF) was calculated as follows: CTFC = Integrated Density – (Area of selected cell x Mean fluorescence of background readings). The parameters for the pEGFR CTCF calculation in Neuro2a Neuro2a-uPAR and Neuro2a-sh-uPAR cells were evaluated using ImageJ; ~~C – EGFR mRNA expression level evaluated using RT-PCR in Neuro2a cells with different uPAR levels; D – Western blot analysis of total EGFR and pEGFR levels, β3-tubulin was used as the loading control. E – a densitometry analysis of the results. Scale bar 20 μm.~~

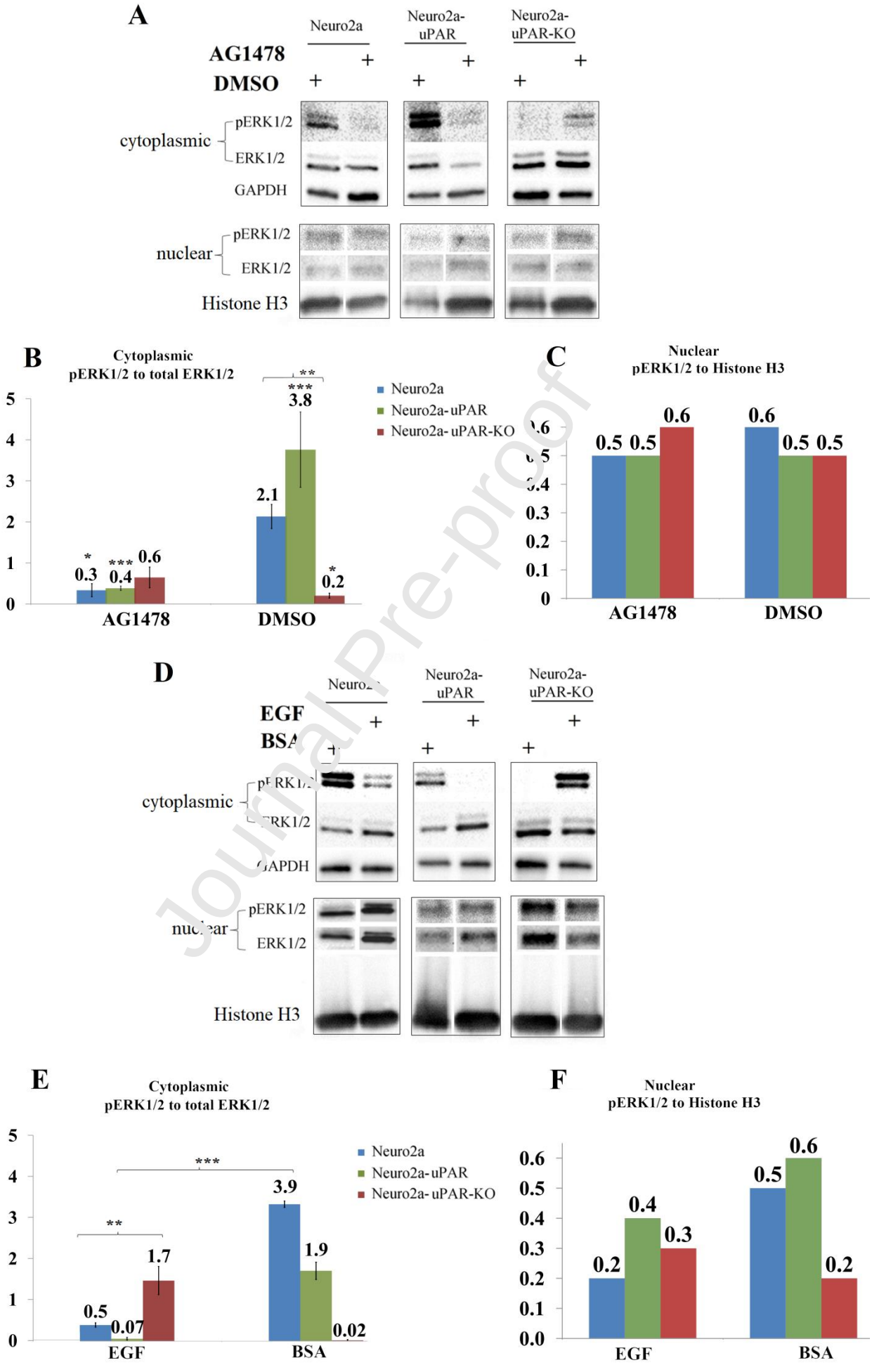
A
Neuro2a
Neuro2a-uPAR
Neuro2a-uPAR-KO
AG1478
DMSO
cytoplasmic
pERK1/2
ERK1/2
GAPDH
nuclear
pERK1/2
ERK1/2
Histone H3
B
Cytoplasmic
pERK1/2 to total ERK1/2
Neuro2a
Neuro2a-uPAR
Neuro2a-uPAR-KO
0.3
0.4
0.6
2.1
3.8
0.2
AG1478
DMSO
C
Nuclear
pERK1/2 to Histone H3
0.5 0.5 0.6
0.6 0.5 0.5
AG1478
DMSO
D
Neuro2a-uPAR
Neuro2a-uPAR-KO
EGF
BSA
cytoplasmic
nuclear
pERK1/2
ERK1/2
Histone H3
E
Cytoplasmic
pERK1/2 to total ERK1/2
Neuro2a
Neuro2a-uPAR
Neuro2a-uPAR-KO
0.5
0.07
1.7
3.9
1.9
0.02
EGF
BSA
F
Nuclear
pERK1/2 to Histone H3
0.2
0.4
0.3
0.5
0.6
0.2
EGF
BSA

Fig. 6. The effect of uPAR expression on the pERK1/2 level in the cytoplasmic and nuclear fractions of Neuro2a cells. Analysis of ERK1/2, pERK1/2, GAPDH and histone H3 levels was performed by Western blot in control Neuro2a cells (Neuro2a), cells with uPAR overexpression (Neuro2a-uPAR) and in Neuro2a with *uPAR* knockout (Neuro2a-uPAR-KO). A – after 1 h incubation with EGFR inhibitor AG1478 (at a concentration of 100 μM) or DMSO (1%) as a control, N=3. B, C – a densitometry analysis of cytoplasmic and nuclear pERK1/2 upon AG1478 or DMSO treatment; D – after 5 min incubation with EGF or BSA as a control (both at a concentration of 50 ng/ml), N=3. E, F – a densitometry analysis of cytoplasmic and nuclear pERK1/2 upon EGF or BSA treatment. GAPDH and histone H3 were used as the loading controls for cytoplasmic and nuclear fractions, respectively. Data are presented as mean values of +/- SEM (N = 3). * $p < 0.05$, ** $p < 0.01$, *** $p < 0.001$ as determined by ANOVA Newman-Keuls test.

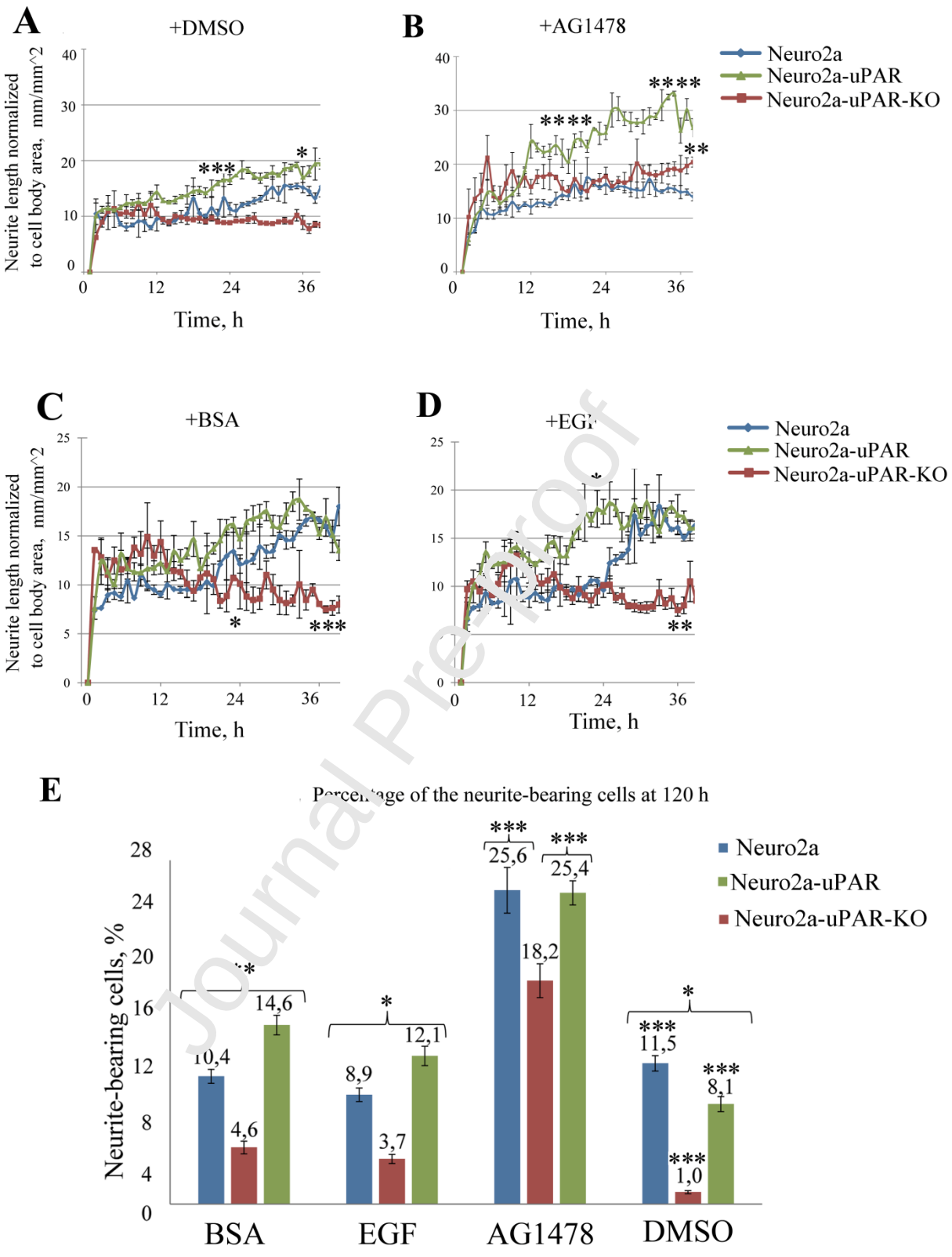

Fig. 7. uPAR expression defines the neurite growth in Neuro2a cells via EGFR activity. The neurite length was analyzed using the IncuCyte® system and the Neurotrack plugin. The data are presented as the length of neurites normalized to the area occupied by the cell bodies (in mm/mm^2). Data are presented as mean +/- SEM (N = 4-5). A – the growth of neurites in control cells (Neuro2a), *uPAR* knockout clone (Neuro2a-uPAR-KO) and uPAR (Neuro2a-uPAR)

overexpressing cells in the presence of DMSO at a concentration of 0.2%; B – in the presence of AG1478 (20 μM). C – in the presence of BSA (50 ng/ml); D – in the presence of EGF (50 ng/ml). E – percentage of the neurite-bearing cells at 120 h. At 24 h *p <0.05 Neuro2a-uPAR versus Neuro2a-uPAR-KO cells; Neuro2a versus Neuro2a-uPAR-KO cells, no statistically significant difference between Neuro2a-uPAR and Neuro2a cells. At 36 h **p <0.01, ***p <0.001 Neuro2a-uPAR versus Neuro2a-uPAR-KO cells; Neuro2a versus Neuro2a-uPAR-KO cells, no difference for Neuro2a-uPAR versus Neuro2a cells. **** p <0.0001 as determined by ANOVA Tukey's test.

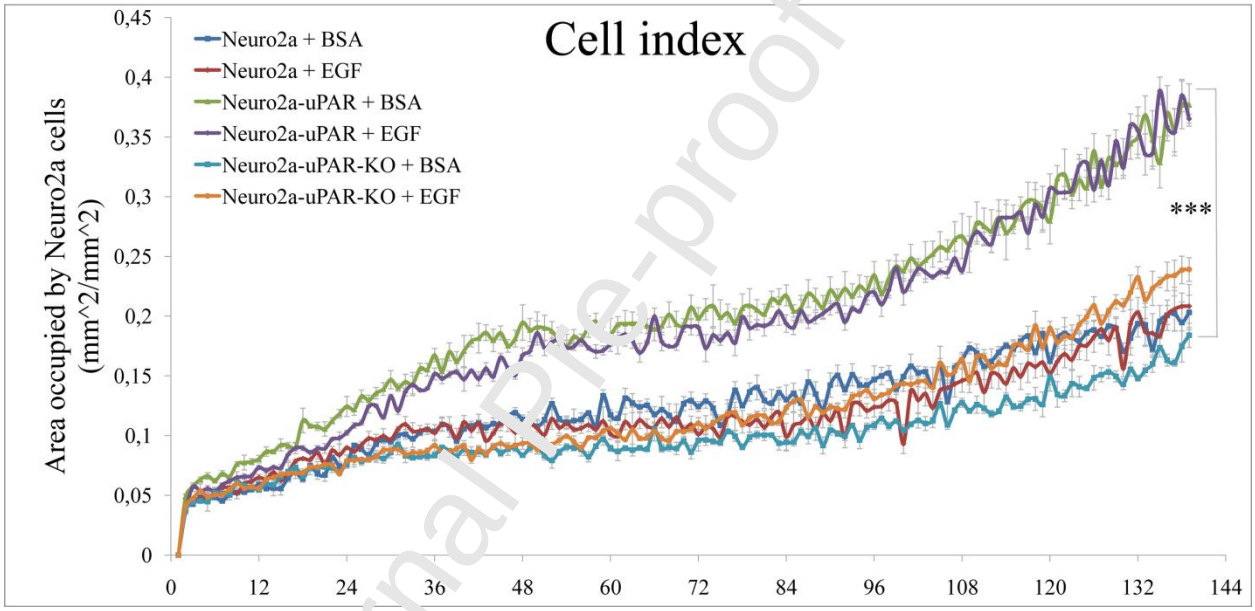

Fig. 8. The dependence of the cell index (the area occupied by Neuro2a cells) with different levels of uPAR expression on EGFR activity. The area occupied by the cell bodies (in mm^2/mm^2) was evaluated in real time using the IncuCyte® system (cell-body cluster mask). Data are presented as mean+/-SEM (N = 4-5 wells per cell type, 100 cells per well). EGF or BSA were administrated at 50 ng/ml each. At 120 h ***p<0.001 Neuro2a-uPAR cells versus Neuro2a and Neuro2a-uPAR-KO regardless of EGF or BSA administration as determined by ANOVA Tukey's test.

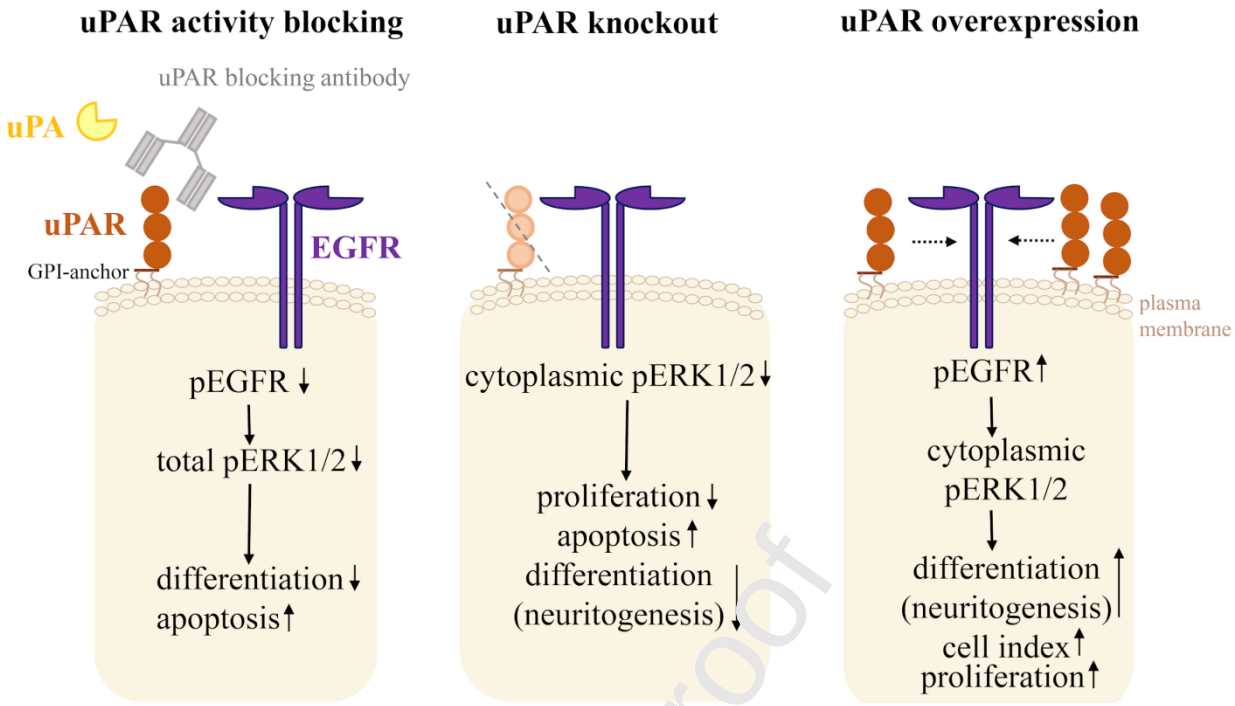

Fig. 9. Schematic diagram of uPAR-mediated signaling pathways and differentiation/neuritogenesis in Neuro2a cells.

(1) Blocking of uPAR activity with specific antibody rapidly decreases phosphorylation of EGFR and its downstream pERK1/2, resulting in a loss of differentiated status (downregulated NeuN expression), enhanced neurite branching [19], reduced survival, DNA damage and induction of apoptosis.

(2) *uPAR* knockout results in downregulated cell differentiation and neuritogenesis (fewer neurites and shorter processes) and decreased cell proliferation [4]. Interestingly, signaling effects in Neuro2a-uPAR-KO cells are different from those in cells with uPAR activity blocked by antibody. In *uPAR* knockout cells total pERK1/2 remains unchanged [4], cytoplasmic pERK1/2 is reduced, and nuclear pERK1/2 is unaffected.

(3) uPAR overexpression leads to activation of EGFR and ERK1/2 and the increase in the cytoplasmic pEGFR and pERK1/2, accompanied by enhanced cell differentiation/neuritogenesis and increased cells index (proliferation or/and survival) [46]. EGF affects only cells overexpressing uPAR and stimulates their neuritogenesis. AG1478, an EGFR inhibitor, has no effect on neurite outgrowth.

References

1. Brodeur G. M. Spontaneous regression of neuroblastoma. // Cell Tissue Res, 2018. Vol. 372, № 2. P. 277-286.

2. Brodeur G. M. Neuroblastoma: biological insights into a clinical enigma. // Nat Rev Cancer, 2003. Vol. 3, № 3. P. 203-216.

3. Nakagawara A. Trk receptor tyrosine kinases: a bridge between cancer and neural development. // Cancer Lett, 2001. Vol. 169, № 2. P. 107-114.

4. Rysenkova K. D. et al. CRISPR/Cas9 nickase mediated targeting of urokinase receptor gene inhibits neuroblastoma cell proliferation. // Oncotarget, 2018. Vol. 9, № 50. P. 29414-29430.

5. Eden G. et al. The urokinase receptor interactome. // Curr Pharm Des, 2011. Vol. 17, № 19. P. 1874-1889.

6. Smith H. W., Marshall C. J. Regulation of cell signalling by uPAR. // Nat Rev Mol Cell Biol, 2010. Vol. 11, № 1. P. 23-36.

7. Evangelopoulos M. E., Weis J., Kruttgen A. Signalling pathways leading to neuroblastoma differentiation after serum withdrawal: HDL blocks neuroblastoma differentiation by inhibition of EGFR. // Oncogene, 2005. Vol. 24, № 2[illegible] P. 3309-3318.

8. Freed D. M. et al. EGFR Ligands Differentially Stabilize Receptor Dimers to Specify Signaling Kinetics. // Cell, 2017. Vol. 171, № 3. P. 683-695 e618.

9. Wilson K. J. et al. Functional selectivity of EGF family peptide growth factors: implications for cancer. // Pharmacol Ther, 2009. Vol. 122, № 1. P. 1-8.

10. Yamada M., Ikeuchi T., Hatanaka H. The neurotrophic action and signalling of epidermal growth factor. // Prog Neurobiol, 1997. Vol. 51, № 1. P. 19-37.

11. Henriksen L. et al. Internalization mechanisms of the epidermal growth factor receptor after activation with different ligands. // PLoS One, 2013. Vol. 8, № 3. P. e58148.

12. Lemarchand E. et al. Stressed neurons protect themselves by a tissue-type plasminogen activator-mediated EGFR-dependent mechanism. // Cell Death Differ, 2016. Vol. 23, № 1. P. 123-131.

13. Wagner B. et al. Neuronal survival depends on EGFR signaling in cortical but not midbrain astrocytes. // EMBO J, 2006. Vol. 25, № 4. P. 752-762.

14. Liu D. et al. EGFR is a transducer of the urokinase receptor initiated signal that is required for in vivo growth of a human carcinoma. // Cancer Cell, 2002. Vol. 1, № 5. P. 445-457.

15. Wei Y. et al. Regulation of integrin function by the urokinase receptor. // Science, 1996. Vol. 273, № 5281. P. 1551-1555.

16. Koshelnick Y. et al. Urokinase receptor is associated with the components of the JAK1/STAT1 signaling pathway and leads to activation of this pathway upon receptor clustering in the human kidney epithelial tumor cell line TCL-598. // J Biol Chem, 1997. Vol. 272, № 45. P. 28563-28567.

17. Bezuidenhout L. et al. Ang-2 and PDGF-BB cooperatively stimulate human peripheral blood monocyte fibrinolysis. // J Leukoc Biol, 2007. Vol. 81, № 6. P. 1496-1503.

18. Farias-Eisner R. et al. Expression of the urokinase plasminogen activator receptor is transiently required during "priming" of PC12 cells in nerve growth factor-directed cellular differentiation. // J Neurosci Res, 2001. Vol. 63, № 4. P. 341-346.

19. Semina E. et al. Urokinase and urokinase receptor participate in regulation of neuronal migration, axon growth and branching. // Eur J Cell Biol, 2016. Vol. 95, № 9. P. 295-310.

20. Merino P. et al. Urokinase-type Plasminogen Activator (uPA) Binding to the uPA Receptor (uPAR) Promotes Axonal Regeneration in the Central Nervous System. // J Biol Chem, 2017. Vol. 292, № 7. P. 2741-2753.

21. Hayden S. M., Seeds N. W. Modulated expression of plasminogen activator system components in cultured cells from dissociated mouse dorsal root ganglia. // J Neurosci, 1996. Vol. 16, № 7. P. 2307-2317.

22. Lino N. et al. uPA-uPAR molecular complex is involved in cell signaling during neuronal migration and neuritogenesis. // Dev Dyn, 2014. Vol. 243, № 5. P. 676-689.

23. Cooper F. et al. Enhancement of Cutaneous Wound Healing by Dsg2 Augmentation of uPAR Secretion. // J Invest Dermatol, 2018. Vol. 138, № 11. P. 2470-2479.

24. Dekkers P. E. et al. Upregulation of monocyte urokinase plasminogen activator receptor during human endotoxemia. // Infect Immun, 2000. Vol. 68, № 4. P. 2156-2160.

25. Mahmood N., Mihalcioiu C., Rabbani S. A. Multifaceted Role of the Urokinase-Type Plasminogen Activator (uPA) and Its Receptor (uPAR): Diagnostic, Prognostic, and Therapeutic Applications. // Front Oncol, 2018. Vol. 8. P. 24.

26. Rubina K. A. et al. Increased expression of uPA, uPAR, and PAI-1 in psoriatic skin and in basal cell carcinomas. // Arch Dermatol Res, 2017. Vol. 309, № 6. P. 433-442.

27. Seetoo D. Q. et al. Quantitative expression of protein markers of plasminogen activation system in prognosis of colorectal cancer. // J Surg Oncol, 2003. Vol. 82, № 3. P. 184-193.

28. Okusa Y. et al. Urokinase type plasminogen activator and its receptor regulate the invasive potential of gastric cancer cell lines. // Int J Oncol, 2000. Vol. 17, № 5. P. 1001-1015. https://doi.org/1010.3892/ijo.1017.1005.1001.

29. Bacchiocchi R. et al. Prognostic value analysis of urokinase-type plasminogen activator receptor in oral squamous cell carcinoma: an immunohistochemical study. // BMC Cancer, 2008. Vol. 8. P. 220.

30. Hildenbrand R. et al. Amplification of the urokinase-type plasminogen activator receptor (uPAR) gene in ductal pancreatic carcinomas identifies a clinically high-risk group. // Am J Pathol, 2009. Vol. 174, № 6. P. 2246-2253.

31. Wang L. et al. Expression of urokinase plasminogen activator and its receptor in advanced epithelial ovarian cancer patients. // Gynecol Oncol, 2009. Vol. 114, № 2. P. 265-272.

32. Almasi C. E. et al. Prognostic significance of urokinase plasminogen activator receptor and its cleaved forms in blood from patients with non-small cell lung cancer. // APMIS, 2009. Vol. 117, № 10. P. 755-761.

33. Seddighzadeh M. et al. Expression of UPA and UPAR is associated with the clinical course of urinary bladder neoplasms. // Int J Cancer, 2002. Vol. 99, № 5. P. 721-726.

34. Giannopoulou I. et al. The prognostic value of the topographic distribution of uPAR expression in invasive breast carcinomas. // Cancer Lett, 2007. Vol. 246, № 1-2. P. 262-267.

35. Ohba K. et al. Expression of urokinase-type plasminogen activator, urokinase-type plasminogen activator receptor and plasminogen activator inhibitors in patients with renal cell carcinoma: correlation with tumor associated macrophage and prognosis. // J Urol, 2005. Vol. 174, № 2. P. 461-465.

36. Aref S. et al. Urokinase plasminogen activator receptor and soluble matrix metalloproteinase-9 in acute myeloid leukemia patients: a possible relation to disease invasion. // Hematology, 2003. Vol. 8, № 6. P. 385-391.

37. Morita Y. et al. Expression of urokinase-type plasminogen activator receptor in hepatocellular carcinoma. // Hepatology, 1997. Vol. 25, № 4. P. 856-861.

38. Kjellman A. et al. Soluble urokinase plasminogen activator receptor as a prognostic marker in men participating in prostate cancer screening. // J Intern Med, 2011. Vol. 269, № 3. P. 299-305.

39. Taubert H. et al. Co-detection of members of the urokinase plasminogen activator system in tumour tissue and serum correlates with a poor prognosis for soft-tissue sarcoma patients. // Br J Cancer, 2010. Vol. 102, № 4. P. 731-737.

40. Buergy D. et al. Urokinase receptor, MMP-1 and MMP-9 are markers to differentiate prognosis, adenoma and carcinoma in thyroid malignancies. // Int J Cancer, 2009. Vol. 125, № 4. P. 894-901.

41. Guerrero J. et al. EGF receptor transactivation by urokinase receptor stimulus through a mechanism involving Src and matrix metalloproteinases. // Exp Cell Res, 2004. Vol. 292, № 1. P. 201-208.

42. Salomon D. S. et al. Epidermal growth factor-related peptides and their receptors in human malignancies. // Crit Rev Oncol Hematol, 1995. Vol. 19, № 3. P. 183-232.

43. Richards K. N. et al. Signaling of ERBB receptor tyrosine kinases promotes neuroblastoma growth in vitro and in vivo. // Cancer, 2010. Vol. 116, № 13. P. 3233-3243.

44. Chiu B., Mirkin B., Madonna M. B. Epidermal growth factor can induce apoptosis in neuroblastoma. // J Pediatr Surg, 2007. Vol. 42, № 3. P. 482-488.

45. Mao J. et al. EGFR/EGFRvIII Dual-Targeting Peptide-Mediated Drug Delivery for Enhanced Glioma Therapy. // ACS Appl Mater Interfaces, 2017. Vol. 9, № 29. P. 24462-24475.

46. Semina E. V. et al. Downregulation of uPAR promotes urokinase translocation into the nucleus and epithelial to mesenchymal transition in neuroblastoma. // J Cell Physiol, 2020.

47. Mirkin B. L., Clark S. H., Zhang C. Inhibition of human neuroblastoma cell proliferation and EGF receptor phosphorylation by gangliosides GM1, GM3, GD1A and GT1B. // Cell Prolif, 2002. Vol. 35, № 2. P. 105-115.

48. Eguchi S. et al. Calcium-dependent epidermal growth factor receptor transactivation mediates the angiotensin II-induced mitogen-activated protein kinase activation in vascular smooth muscle cells. // J Biol Chem, 1998. Vol. 273, № 15. P. 8890-8896.

49. Chen H., Liu B., Neufeld A. H. Epidermal growth factor receptor in adult retinal neurons of rat, mouse, and human. // J Comp Neurol, 2007. Vol. 500, № 2. P. 299-310.

50. Gusel'nikova V. V., Korzhevskiy D. E. NeuN As a Neuronal Nuclear Antigen and Neuron Differentiation Marker. // Acta Naturae, 2015. Vol. 7, № 2. P. 42-47.

51. Wee P., Wang Z. Epidermal Growth Factor Receptor Cell Proliferation Signaling Pathways. // Cancers (Basel), 2017. Vol. 9, № 5.

52. Ray Chaudhuri A., Nussenzweig A. The multifaceted roles of PARP1 in DNA repair and chromatin remodelling. // Nat Rev Mol Cell Biol, 2017. Vol. 18, № 10. P. 610-621.

53. Nicholson D. W. et al. Identification and inhibition of the ICE/CED-3 protease necessary for mammalian apoptosis. // Nature, 1995. Vol. 376, № 6535. P. 37-43.

54. Gyori B. M. et al. OpenComet: an automated tool for comet assay image analysis. // Redox Biol, 2014. Vol. 2. P. 457-465.

55. Gedik C. M., Ewen S. W., Collins A. R. Single-cell gel electrophoresis applied to the analysis of UV-C damage and its repair in human cells. // Int J Radiat Biol, 1992. Vol. 62, № 3. P. 313-320.

56. Ellis A. G. et al. Preclinical analysis of the analinoquinazoline AG1478, a specific small molecule inhibitor of EGF receptor tyrosine kinase. // Biochem Pharmacol, 2006. Vol. 71, № 10. P. 1422-1434.

57. Wortzel I., Seger R. The ERK Cascade: Distinct Functions within Various Subcellular Organelles. // Genes Cancer, 2011. Vol. 2, № 3. P. 195-209.

58. Michailovici I. et al. Nuclear to cytoplasmic shuttling of ERK promotes differentiation of muscle stem/progenitor cells. // Development, 2014. Vol. 141, № 13. P. 2611-2620.

59. Douglas M. R. et al. Off-target effects of epidermal growth factor receptor antagonists mediate retinal ganglion cell disinhibited axon growth. // Brain, 2009. Vol. 132, № Pt 11. P. 3102-3121.

60. Fan K. Preferential synthesis of differentiation related cytoplasmic proteins in low-serum adapted differentiated glioma cells. // Neurosci Lett, 1983. Vol. 41, № 1-2. P. 205-210.

61. Conti L. et al. Shc signaling in differentiating neural progenitor cells. // Nat Neurosci, 2001. Vol. 4, № 6. P. 579-586.

62. Howard M. K. et al. Cell cycle arrest of proliferating neuronal cells by serum deprivation can result in either apoptosis or differentiation. // J Neurochem, 1993. Vol. 60, № 5. P. 1783-1791.

63. Chan W. S. et al. Differential regulation of proliferation and neuronal differentiation in adult rat spinal cord neural stem/progenitors by ERK1/2, Akt, and PLCgamma. // Front Mol Neurosci, 2013. Vol. 6. P. 23.

64. Li Z., Theus M. H., Wei L. Role of ERK 1/2 signaling in neuronal differentiation of cultured embryonic stem cells. // Dev Growth Differ, 2006. Vol. 48, № 8. P. 513-523.

65. Chen S. et al. Neuroprotective Role of the PI3 Kinase/Akt Signaling Pathway in Zebrafish. // Front Endocrinol (Lausanne), 2017. Vol. 8. P. 21.

66. Pellegrino M. J., Stork P. J. Sustained activation of extracellular signal-regulated kinase by nerve growth factor regulates c-fos protein stabilization and transactivation in PC12 cells. // J Neurochem, 2006. Vol. 99, № 6. P. 1480-1493.

67. Wang X. et al. Essential role of ERK activation in neurite outgrowth induced by alpha-lipoic acid. // Biochim Biophys Acta, 2011. Vol. 1813, № 5. P. 827-838.

68. Ma Z. et al. Endogenously produced urokinase-type plasminogen activator is a major determinant of the basal level of activated ERK/MAP kinase and prevents apoptosis in MDA-MB-231 breast cancer cells. // J Cell Sci, 2001. Vol. 114, № Pt 18. P. 3387-3396.

69. Jo M. et al. Urokinase receptor primes cells to proliferate in response to epidermal growth factor. // Oncogene, 2007. Vol. 26, № 18. P. 2585-2594.

70. Lopez J. et al. Src tyrosine kinase inhibits apoptosis through the Erk1/2- dependent degradation of the death accelerator Bik. // Cell Death Differ, 2012. Vol. 19, № 9. P. 1459-1469.

71. Iqbal Hossain M. et al. Dual role of Src kinase in governing neuronal survival. // Brain Res, 2015. Vol. 1594. P. 1-14.

72. Tippett L. J. et al. Striosomes and mood dysfunction in Huntington's disease. // Brain, 2007. Vol. 130, № Pt 1. P. 206-221.

73. Butler T. R. et al. Selective vulnerability of hippocampal cornu ammonis 1 pyramidal cells to excitotoxic insult is associated with the expression of polyamine-sensitive N-methyl-D-asparate-type glutamate receptors. // Neuroscience, 2010. Vol. 165, № 2. P. 525-534.

74. Chaitanya G. V., Steven A. J., Babu P. P. PARP-1 cleavage fragments: signatures of cell-death proteases in neurodegeneration. // Cell Commun Signal, 2010. Vol. 8. P. 31.

75. Bhaskara V. K. et al. Comparative status of activated ERK1/2 and PARP cleavage in human gliomas. // Neuropathology, 2005. Vol. 25, № 1. P. 48-53.

76. Chaitanya G. V., Babu P. P. Differential PARP cleavage: an indication of heterogeneous forms of cell death and involvement of multiple proteases in the infarct of focal cerebral ischemia in rat. // Cell Mol Neurobiol, 2009. Vol. 29, № 4. P. 563-573.

77. Gilliams-Francis K. L., Quaye A. A., Naegele J. R. PARP cleavage, DNA fragmentation, and pyknosis during excitotoxin-induced neuronal death. // Exp Neurol, 2003. Vol. 184, № 1. P. 359-372.

78. Roepstorff K. et al. Differential effects of EGFR ligands on endocytic sorting of the receptor. // Traffic, 2009. Vol. 10, № 8. P. 1115-1127.

79. Lenormand P. et al. Growth factors induce nuclear translocation of MAP kinases (p42mapk and p44mapk) but not of their activator MAP kinase kinase (p45mapkk) in fibroblasts. // J Cell Biol, 1993. Vol. 122, № 5. P. 1079-1088.

80. Caunt C. J., McArdle C. A. Stimulus-induced uncoupling of extracellular signal-regulated kinase phosphorylation from nuclear localization is dependent on docking domain interactions. // J Cell Sci, 2010. Vol. 123, № Pt 24. P. 4310-4320.

81. Jo M. et al. Epidermal growth factor receptor-dependent and -independent cell-signaling pathways originating from the urokinase receptor. // J Biol Chem, 2003. Vol. 278, № 3. P. 1642-1646.

82. Li H. et al. Amino-terminal fragment of urokinase inhibits tumor cell invasion in vitro and in vivo: respective contribution of the urokinase plasminogen activator receptor-dependent or -independent pathway. // Hum Gene Ther, 2005. Vol. 16, № 10. P. 1157-1167.

83. Kobayashi H. et al. Inhibition of metastasis of Lewis lung carcinoma by a synthetic peptide within growth factor-like domain of urokinase in the experimental and spontaneous metastasis model. // Int J Cancer, 1994. Vol. 57, № 5. P. 727-733.

84. Rabbani S. A., Gladu J. Urokinase receptor antibody can reduce tumor volume and detect the presence of occult tumor metastases in vivo. // Cancer Res, 2002. Vol. 62, № 8. P. 2390-2397.

85. Knor S. et al. Development and evaluation of peptidic ligands targeting tumour-associated urokinase plasminogen activator receptor (uPAR) for use in alpha-emitter therapy for disseminated ovarian cancer. // Eur J Nucl Med Mol Imaging, 2008. Vol. 35, № 1. P. 53-64.

86. Raghu H. et al. uPA and uPAR shRNA inhibit angiogenesis via enhanced secretion of SVEGFR1 independent of GM-CSF but dependent on TIMP-1 in endothelial and glioblastoma cells. // Mol Oncol, 2012. Vol. 6, № 1. P. 33-47.

CRediT author statement

Rysenkova Karina D.: Methodology, Investigation, Validation, Formal analysis, Visualization, Writing - Original Draft. Klimovich Polina S.: Investigation. Shmakova Anna A.: Validation, Formal analysis. Karagyaur Maxim N.: Investigation. Ivanova Karina A.: Validation, Writing - Original Draft. Alexandrushkina Natalya A.: Investigation. Tkachuk Vsevolod A.: Conceptualization, Funding acquisition. Rubina Kseniya A.: Conceptualization, Supervision, Visualization, Writing - Reviewing and Editing. Semina Ekaterina V.: Methodology, Investigation, Visualization, Conceptualization, Project administration, Funding acquisition.

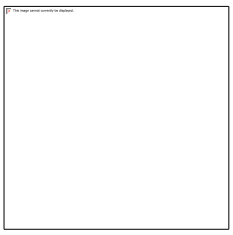

Highlights

- uPAR is an important regulator of neuroblastoma cell survival and differentiation
- uPAR is upstream of the EGFR/ERK1/2 signaling pathway
- EGFR/ERK1/2 controls cell survival in the absence of uPAR
- EGFR/ERK1/2 promotes neurite growth in uPAR-expressing cells